

APPENDIX 3. HIGHLIGHTED ARTICLES PUBLISHED IN 2007



GEOPHYSICAL RESEARCH LETTERS, VOL. 34, L23811, doi:10.1029/2007GL031538, 2007

Cooling of the Atlantic by Saharan dust

K. M. Lau¹ and K. M. Kim²

Received 3 August 2007; revised 19 October 2007; accepted 6 November 2007; published 8 December 2007.

[1] Using aerosol optical depth, sea surface temperature, top-of-the-atmosphere solar radiation flux, and oceanic mixed-layer depth from diverse data sources that include NASA satellites, NCEP reanalysis, *in situ* observations, as well as long-term dust records from Barbados, we examine the possible relationships between Saharan dust and Atlantic sea surface temperature. Results show that the estimated anomalous cooling pattern of the Atlantic during June 2006 relative to June 2005 due to attenuation of surface solar radiation by Saharan dust remarkably resemble observations, accounting for approximately 30–40% of the observed change in sea surface temperature. Historical data analysis show that there is a robust negative correlation between atmospheric dust loading and Atlantic SST consistent with the notion that increased (decreased) Saharan dust is associated with cooling (warming) of the Atlantic during the early hurricane season (July–August–September). **Citation:** Lau, K. M., and K. M. Kim (2007), Cooling of the Atlantic by Saharan dust, *Geophys. Res. Lett.*, *34*, L23811, doi:10.1029/2007GL031538.

1. Introduction

[2] An estimated amount of 60–200 million tons of dust particles are lifted annually from the Saharan desert surface and transported westward by the easterly winds over the Atlantic Ocean [Prospero and Lamb, 2003]. During the peak season of June through August, airborne dust particles reach the western Atlantic and Caribbean, and can be detected as far west as Florida, and the Gulf of Mexico [Colarco *et al.*, 2003; Wong *et al.*, 2006]. Saharan dusts have been shown to affect the development of clouds and precipitation over oceanic areas across the Atlantic, as well as modulating thunderstorm activities over the Caribbean, and the southeast US [Kaufman *et al.*, 2005; Sassen *et al.*, 2003]. Hot dry air, known as the Saharan Air Layer (SAL), which often accompanies Saharan dust outbreaks, can suppress tropical cyclogenesis and inhibit Atlantic hurricane formation [Dunion and Velden, 2004; Wu, 2007]. Studies have also found significant positive correlation between dust cover and Atlantic tropical cyclone days [Evan *et al.*, 2006].

[3] Recently Lau and Kim [2007a] found significant increase in Saharan dust and reduction of sea surface temperature (SST) over the West Atlantic and Caribbean region during the hurricane season, June through November, of

2006 compared to 2005. They argued that the attenuation of solar radiation reaching the ocean surface by excessive Saharan dust in June–July, 2006 (relative to 2005) may have been instrumental in initiating the rapid cooling of the entire Atlantic Ocean. The cooling subsequent metastasized through atmospheric-oceanic coupled feedback to become a part of an altered climate state in the North Atlantic and West Africa regions unfavorable for hurricane formation. In a subsequent exchange [Evan, 2007; Lau and Kim, 2007b], issues were raised regarding the magnitude of the difference in atmospheric dust loading, and the degree to which solar attenuation effect by dust could lower Atlantic SST. In this paper, we present observation-based estimates of possible large-scale cooling of the Atlantic by Saharan dust attenuation effect for 2006 relative to 2005, and examine statistical dust-SST relationships based on long-term historical records.

[4] The data used for this study are drawn from a wide range of independent sources, including daily Aerosol-Index (AI) [Hsu *et al.*, 1999] for absorbing aerosols (dust and black carbon) from the Ozone Monitoring Instrument (OMI), aerosol optical depth (AOD) from the Moderate Resolution Imaging Spectroradiometer (MODIS) [Remer *et al.*, 2005], daily sea surface temperature from Tropical Rainfall Measuring Mission Microwave Imager (TMI), top-of-the atmosphere solar radiation from the National Center for Environmental Prediction (NCEP) reanalysis data, and climatological oceanic mixed layer depth from the Laboratoire d'Océanographie et du Climat: Expérimentation et Approches Numériques (LOCEAN). Also used for the historical data analysis are long-term data from the Barbados dust record [Prospero and Nees, 1986], and the SST record from the Hadley Center [Rayner *et al.*, 2003].

2. Results

2.1. Dust and SST Variation During 2005–2006

[5] From the daily variation (smoothed by a 5-day running mean) of dust loading (OMI-AI) and SST over the Western Atlantic/Caribbean region (70°W–40°W, 15°N–30°N) in 2006, (shown as the deviation from 2005 in Figure 1), dust loading is clearly higher for most of the year in 2006 compared to 2005 (Figure 1a). The dust loading shows large fluctuations from June through September, reflecting the dynamical nature of the dust outbreak and transport processes. This region experienced episodic cooling in SST throughout 2006 (Figure 1b), with two significant episodes in mid-March through May, which seemed to follow two dust events (Figure 1a) during the same period. The most pronounced cooling occurred in mid-June, about one-to-two weeks after the major dust event in June. The cooling rapidly reached its maximum in late June and mid-July, and lasted through the end of September. Given that dust outbreaks and loadings are highly dependent on fast atmospheric processes, and SST on relatively slow ocean processes, any relationship

¹Laboratory for Atmospheres, NASA Goddard Space Flight Center, Greenbelt, Maryland, USA.

²Goddard Earth Science and Technology Center, University of Maryland Baltimore County, Baltimore, Maryland, USA.

A Numerical Study of Hurricane Erin (2001). Part II: Shear and the Organization of Eyewall Vertical Motion

SCOTT A. BRAUN

Mesoscale Atmospheric Processes Branch, Laboratory for Atmospheres, NASA Goddard Space Flight Center, Greenbelt, Maryland

LIGUANG WU

Goddard Earth Science and Technology Center, University of Maryland, Baltimore County, Baltimore, Maryland

(Manuscript received 11 January 2006, in final form 19 June 2006)

ABSTRACT

A high-resolution numerical simulation of Hurricane Erin (2001) is used to examine the organization of vertical motion in the eyewall and how that organization responds to a large and rapid increase in the environmental vertical wind shear and subsequent decrease in shear. During the early intensification period, prior to the onset of significant shear, the upward motion in the eyewall was concentrated in small-scale convective updrafts that formed in association with regions of concentrated vorticity (herein termed mesovortices) with no preferred formation region around the eyewall. Asymmetric flow within the eye was weak. As the shear increased, an azimuthal wavenumber-1 asymmetry in storm structure developed with updrafts tending to occur on the downshear to downshear-left side of the eyewall. Continued intensification of the shear led to increasing wavenumber-1 asymmetry, large vortex tilt, and a change in eyewall structure and vertical motion organization. During this time, the eyewall structure was dominated by a vortex couplet with a cyclonic (anticyclonic) vortex on the downtilt-left (downtilt-right) side of the eyewall and strong asymmetric flow across the eye that led to strong mixing of eyewall vorticity into the eye. Upward motion was concentrated over an azimuthally broader region on the downtilt side of the eyewall, upstream of the cyclonic vortex, where low-level environmental inflow converged with the asymmetric outflow from the eye. As the shear diminished, the vortex tilt and wavenumber-1 asymmetry decreased, while the organization of updrafts trended back toward that seen during the weak shear period. Based upon the results for the Erin case, as well as that for a similar simulation of Hurricane Bonnie (1998), a conceptual model is developed for the organization of vertical motion in the eyewall as a function of the strength of the vertical wind shear. In weak to moderate shear, higher wavenumber asymmetries associated with eyewall mesovortices dominate the wavenumber-1 asymmetry associated with the shear so that convective-scale updrafts form when the mesovortices move into the downtilt side of the eyewall and dissipate on the uptilt side. Under strong shear conditions, the wavenumber-1 asymmetry, characterized by a prominent vortex couplet in the eyewall, dominates the vertical motion organization so that mesoscale ascent (with embedded convection) occurs over an azimuthally broader region on the downtilt side of the eyewall. Further research is needed to determine if these results apply more generally.

1. Introduction

The National Aeronautics and Space Administration (NASA) Tropical Rainfall Measuring Mission (TRMM) satellite has proven to be a valuable tool for the study of precipitation in hurricanes. Lonfat et al. (2004) used rainfall estimates from the TRMM Micro-

wave Imager (TMI) to examine the climatological rainfall characteristics of hurricanes with emphases on the variations with respect to storm intensity and location (different ocean basins) and on asymmetries in rainfall structure. Cecil et al. (2002) and Cecil and Zipser (2002) examined TRMM radar, TMI, and lightning data in hurricanes and found that the precipitation characteristics were very similar to nonhurricane tropical oceanic precipitation. The hurricane outer rainbands produced more lightning per unit area than the eyewall and inner rainbands, as well as other tropical oceanic convection, and were proposed to be a pre-

Corresponding author address: Dr. Scott Braun, Mesoscale Atmospheric Processes Branch, NASA GSFC, Code 613.1, Greenbelt, MD 20771.
E-mail: scott.a.braun@nasa.gov

DOI: 10.1175/MWR3336.1

MWR3336

Tropical Rainfall Variability on Interannual-to-Interdecadal and Longer Time Scales Derived from the GPCP Monthly Product

GUOJUN GU

*Goddard Earth Sciences and Technology Center, University of Maryland, Baltimore County, Baltimore, and
Laboratory for Atmospheres, NASA Goddard Space Flight Center, Greenbelt, Maryland*

ROBERT F. ADLER

Laboratory for Atmospheres, NASA Goddard Space Flight Center, Greenbelt, Maryland

GEORGE J. HUFFMAN

Science Systems and Applications Inc., and Laboratory for Atmospheres, NASA Goddard Space Flight Center, Greenbelt, Maryland

SCOTT CURTIS

Department of Geography, East Carolina University, Greenville, North Carolina

(Manuscript received 15 March 2006, in final form 6 December 2006)

ABSTRACT

Global and large regional rainfall variations and possible long-term changes are examined using the 27-yr (1979–2005) Global Precipitation Climatology Project (GPCP) monthly dataset. Emphasis is placed on discriminating among variations due to ENSO, volcanic events, and possible long-term climate changes in the Tropics. Although the global linear change of precipitation in the dataset is near zero during the time period, an increase in tropical rainfall is noted in the dataset, with a weaker decrease over Northern Hemisphere middle latitudes. Focusing on the Tropics (25°S–25°N), the dataset indicates an upward linear change ($0.06 \text{ mm day}^{-1} \text{ decade}^{-1}$) and a downward linear change ($-0.01 \text{ mm day}^{-1} \text{ decade}^{-1}$) over tropical ocean and land, respectively. This corresponds to an about 5.5% increase (ocean) and 1% decrease (land) during the entire 27-yr time period. The year 2005 has the largest annual tropical total precipitation (land plus ocean) for the GPCP record. The five highest years are (in descending order) 2005, 2004, 1998, 2003, and 2002. For tropical ocean the five highest years are 1998, 2004, 2005, 2002, and 2003.

Techniques are applied to isolate and quantify variations due to ENSO and two major volcanic eruptions during the time period (El Chichón, March 1982; Mount Pinatubo, June 1991) in order to examine longer-time-scale changes. The ENSO events generally do not impact the tropical total rainfall, but rather induce significant anomalies with opposite signs over tropical land and ocean. The impact of the two volcanic eruptions is estimated to be about a 5% reduction in tropical rainfall over both land and ocean. A modified dataset (with ENSO and volcano effects removed) retains the same approximate linear change slopes, but with reduced variances, thereby increasing the statistical significance levels associated with the long-term rainfall changes in the Tropics. However, although care has been taken to ensure that this dataset is as homogeneous as possible, firm establishment of the existence of the discussed changes as long-term trends may require continued analysis of the input datasets and a lengthening of the observation period.

1. Introduction

Exploring global climate variability and change has an immense environmental and societal significance

(e.g., Kumar et al. 2004). Previous studies showed interannual variability and interdecadal/longer-term changes in various climate components, for example, surface air temperature, sea surface temperature (SST), land rainfall, etc., specifically during recent decades (e.g., Cane et al. 1997; Chen et al. 2002; Simmons et al. 2004). The El Niño–Southern Oscillation (ENSO) generally dominates the global variability on interannual

Corresponding author address: Guojun Gu, NASA GSFC, Code 613.1, Greenbelt, MD 20771.
E-mail: ggu@agnes.gsfc.nasa.gov

DOI: 10.1175/JCLI4227.1

© 2007 American Meteorological Society

NASA'S TROPICAL CLOUD SYSTEMS AND PROCESSES EXPERIMENT

Investigating Tropical Cyclogenesis and Hurricane Intensity Change

BY J. HALVERSON, M. BLACK, S. BRAUN, D. CECIL, M. GOODMAN, A. HEYMSFIELD, G. HEYMSFIELD,
R. HOOD, T. KRISHNAMURTI, G. MCFARQUHAR, M. J. MAHONEY, J. MOLINARI, R. ROGERS, J. TURK,
C. VELDEN, D.-L. ZHANG, E. ZIPSER, AND R. KAKAR

High altitude research flights during the active 2005 Atlantic and eastern Pacific hurricane season yielded interesting and surprising observations, both within and above the clouds.

B **ACKGROUND AND MOTIVATION FOR TCSP.** A key mandate of the National Aeronautics and Space Administration's (NASA's) Weather Focus Area is to investigate high-impact weather events, such as tropical cyclones, through a combination of new and improved space-based observations, high-altitude research aircraft, and sophisticated numerical models to improve the understanding

and predictability of weather, climate, and natural hazards. One of the areas of tropical meteorology that remains elusive to both understanding and prediction is the genesis and intensification of tropical cyclones. The processes by which tropical disturbances develop into depressions, storms, or hurricanes (termed tropical cyclogenesis) remain one of the outstanding and fascinating research topics in meteorology. The

AFFILIATIONS: HALVERSON—Joint Center for Earth Systems Technology, University of Maryland, Baltimore County, Baltimore, Maryland; BLACK AND ROGERS—NOAA/Hurricane Research Division, Miami, Florida; BRAUN AND G. HEYMSFIELD—NASA Goddard Space Flight Center, Greenbelt, Maryland; CECIL—Earth System Science Center, University of Alabama, Huntsville, Huntsville, Alabama; GOODMAN AND HOOD—NASA Marshall Space Flight Center, Huntsville, Alabama; A. HEYMSFIELD—University Center for Atmospheric Research, Boulder, Colorado; KRISHNAMURTI—The Florida State University, Tallahassee, Florida; MCFARQUHAR—University of Illinois at Urbana—Champaign, Urbana, Illinois; MAHONEY—Jet Propulsion Laboratory, California Institute of Technology, Pasadena, California; MOLINARI—University at Albany, State University of New York, Albany, New York; TURK—Naval Research Laboratory, Washington, DC; VELDEN—University of Wisconsin—Madison—

Cooperative Institute for Meteorological Satellite Studies, Madison, Wisconsin; ZHANG—University of Maryland, College Park, College Park, Maryland; ZIPSER—University of Utah, Salt Lake City, Utah; KAKAR—NASA Headquarters Science Mission Directorate, Washington, DC.

CORRESPONDING AUTHOR: Dr. Jeffrey B. Halverson, JCET/UMBC, 5523 Research Park Dr., Suite 320, Baltimore, MD 21228
E-mail: jeffhalv@umbc.edu

The abstract for this article can be found in this issue, following the table of contents.

DOI: 10.1175/BAMS-88-6-867

In final form 18 December 2006
©2007 American Meteorological Society



A first approach to global runoff simulation using satellite rainfall estimation

Yang Hong,^{1,2,3} Robert F. Adler,¹ Faisal Hossain,⁴ Scott Curtis,⁵ and George J. Huffman^{1,6}

Received 14 November 2006; revised 14 May 2007; accepted 23 May 2007; published 11 August 2007.

[1] Motivated by the recent increasing availability of global remote sensing data for estimating precipitation and describing land surface characteristics, this note reports an approximate assessment of quasi-global runoff computed by incorporating satellite rainfall data and other remote sensing products in a relatively simple rainfall-runoff simulation approach: the Natural Resources Conservation Service (NRCS) runoff curve number (CN) method. Using an antecedent precipitation index (API) as a proxy of antecedent moisture conditions, this note estimates time-varying NRCS-CN values determined by the 5-day normalized API. Driven by a multiyear (1998–2006) Tropical Rainfall Measuring Mission Multi-satellite Precipitation Analysis, quasi-global runoff was retrospectively simulated with the NRCS-CN method and compared to Global Runoff Data Centre data at global and catchment scales. Results demonstrated the potential for using this simple method when diagnosing runoff values from satellite rainfall for the globe and for medium to large river basins. This work was done with the simple NRCS-CN method as a first-cut approach to understanding the challenges that lie ahead in advancing the satellite-based inference of global runoff. We expect that the successes and limitations revealed in this study will lay the basis for applying more advanced methods to capture the dynamic variability of the global hydrologic process for global runoff monitoring in real time. The essential ingredient in this work is the use of global satellite-based rainfall estimation.

Citation: Hong, Y., R. F. Adler, F. Hossain, S. Curtis, and G. J. Huffman (2007), A first approach to global runoff simulation using satellite rainfall estimation, *Water Resour. Res.*, 43, W08502, doi:10.1029/2006WR005739.

1. Introduction

[2] Many hydrological models have been introduced in the hydrological literature to predict runoff [Singh, 1995], but few of these have become common planning or decision-making tools [Choi *et al.*, 2002], either because the data requirements are substantial or because the modeling processes are too complicated for operational application. On the other hand, progress in regional or global rainfall-runoff simulation has been constrained by the difficulty of measuring spatiotemporal variability of the primary causative factor, i.e., rainfall fluxes, continuously over space and time. Building on progress in remote sensing technology, researchers have improved the accuracy, coverage, and resolution of rainfall estimates by combining imagery from infrared, passive microwave, and space-borne radar sensors

[Adler *et al.*, 2003]. Today remote sensing imagery acquired and processed in real time can provide near-real-time rainfall at hydrologically relevant spatiotemporal scales (tens of kilometers and subdaily [Hong *et al.*, 2005; Huffman *et al.*, 2007; Joyce *et al.*, 2004; Sorooshian *et al.*, 2000; Turk and Miller, 2005]). Over much of the globe, remote sensing precipitation estimates are the only available source of rainfall information, particularly in real time. Correspondingly, remote sensing has increasingly become a viable data source to augment the conventional hydrological rainfall-runoff simulation, especially for inaccessible regions or complex terrains, because remotely sensed imageries are able to monitor precipitation and identify land surface characteristics such as topography, stream network, land cover, vegetation, etc. Artan *et al.* [2007] demonstrated the improved performance of remotely sensed precipitation data in hydrologic modeling when the hydrologic model was recalibrated with satellite data rather than gauge rainfall over four subbasins of the Nile and Mekong rivers.

[3] Motivated by the recent increasing availability of global remote sensing data for estimating precipitation and describing land surface characteristics, this note attempts to obtain a ballpark assessment of global runoff by incorporating satellite rainfall data and other remote sensing products through a relatively simple rainfall-runoff simulation approach: the United States Natural Resources Conservation Service (NRCS) runoff curve number (CN) method [Natural Resources Conservation Service (NRCS), 1986; Burges *et al.*, 1998]. Its simplicity is especially critical for

¹Laboratory for Atmospheres, NASA Goddard Space Flight Center, Greenbelt, Maryland, USA.

²Now at School of Civil Engineering and Environmental Sciences, University of Oklahoma, Norman, Oklahoma, USA.

³Formerly at Goddard Earth Science Technology Center, University of Maryland Baltimore County, Baltimore, Maryland, USA.

⁴Department of Civil and Environmental Engineering, Tennessee Technological University, Cookeville, Tennessee, USA.

⁵Department of Geography, East Carolina University, Greenville, North Carolina, USA.

⁶Science Systems and Applications, Inc., Lanham, Maryland, USA.

The TRMM Multisatellite Precipitation Analysis (TMPA): Quasi-Global, Multiyear, Combined-Sensor Precipitation Estimates at Fine Scales

GEORGE J. HUFFMAN,^{*,+} ROBERT F. ADLER,^{*} DAVID T. BOLVIN,^{*,+} GUOJUN GU,^{*,#} ERIC J. NELKIN,^{*,+} KENNETH P. BOWMAN,[@] YANG HONG,^{*,#} ERICH F. STOCKER,[&] AND DAVID B. WOLFF^{*,+}

^{*}Laboratory for Atmospheres, NASA GSFC, Greenbelt, Maryland

⁺Science Systems and Applications, Inc., Lanham, Maryland

[#]Goddard Earth Sciences and Technology Center, University of Maryland, Baltimore County, Baltimore, Maryland

[@]Texas A&M University, College Station, Texas

[&]Global Change Data Center, NASA GSFC, Greenbelt, Maryland

(Manuscript received 8 March 2006, in final form 22 June 2006)

ABSTRACT

The Tropical Rainfall Measuring Mission (TRMM) Multisatellite Precipitation Analysis (TMPA) provides a calibration-based sequential scheme for combining precipitation estimates from multiple satellites, as well as gauge analyses where feasible, at fine scales ($0.25^\circ \times 0.25^\circ$ and 3 hourly). TMPA is available both after and in real time, based on calibration by the TRMM Combined Instrument and TRMM Microwave Imager precipitation products, respectively. Only the after-real-time product incorporates gauge data at the present. The dataset covers the latitude band 50°N – 50°S for the period from 1998 to the delayed present. Early validation results are as follows: the TMPA provides reasonable performance at monthly scales, although it is shown to have precipitation rate-dependent low bias due to lack of sensitivity to low precipitation rates over ocean in one of the input products [based on Advanced Microwave Sounding Unit-B (AMSU-B)]. At finer scales the TMPA is successful at approximately reproducing the surface observation-based histogram of precipitation, as well as reasonably detecting large daily events. The TMPA, however, has lower skill in correctly specifying moderate and light event amounts on short time intervals, in common with other finescale estimators. Examples are provided of a flood event and diurnal cycle determination.

1. Introduction

Precipitation displays small-scale variability and highly nonnormal statistical behavior that requires frequent, closely spaced observations for adequate representation. Such observations are not possible through surface-based measurements over much of the globe, particularly in oceanic, remote, or developing regions. Consequently, researchers have come to depend on suites of sensors flying on a variety of satellites over the last 25+ years for the majority of the information used to estimate precipitation on a global basis. While it is possible to create such estimates solely from one type of sensor, researchers have increasingly moved to using combinations of sensors in an attempt to improve accuracy, coverage, and resolution. The first such combi-

nations were performed at a relatively coarse scale to ensure reasonable error characteristics. For example, the Global Precipitation Climatology Project (GPCP) satellite–gauge (SG) combination is computed on a monthly $2.5^\circ \times 2.5^\circ$ latitude–longitude grid (Huffman et al. 1997; Adler et al. 2003). Subsequently, the scientific community requested that the estimates be made available at finer scale, even at the cost of higher uncertainties. Finer-scale products initiated by the GPCP include the Pentad (Xie et al. 2003) and One-Degree Daily (Huffman et al. 2001) combination estimates of precipitation. Other research groups have introduced a number of finescale estimates in the past several years that are now in quasi-operational production (see Huffman 2005), including the Climate Prediction Center (CFC) morphing algorithm (CMORPH; Joyce et al. 2004), the Naval Research Laboratory Global Blended-Statistical Precipitation Analysis (NRLgeo; Turk and Miller 2005), the Passive Microwave-Calibrated Infrared algorithm (PMIR; Kidd et al. 2003), and the Precipitation Estimation from Remotely Sensed Informa-

Corresponding author address: George J. Huffman, NASA GSFC, Code 613.1, Greenbelt, MD 20771.
E-mail: huffman@agnes.gsfc.nasa.gov

DOI: 10.1175/JHM560.1

© 2007 American Meteorological Society

JHM560

Improving Simulations of Convective Systems from TRMM LBA: Easterly and Westerly Regimes

S. LANG,* W.-K. TAO,+ R. CIFELLI,# W. OLSON,@ J. HALVERSON,@ S. RUTLEDGE,#
AND J. SIMPSON+

*Laboratory for Atmospheres, NASA Goddard Space Flight Center, Greenbelt, and Science Systems and Applications, Inc.,
Lanham, Maryland

+Laboratory for Atmospheres, NASA Goddard Space Flight Center, Greenbelt, Maryland

#Department of Atmospheric Science, Colorado State University, Fort Collins, Colorado

@Laboratory for Atmospheres, NASA Goddard Space Flight Center, Greenbelt, and Joint Center for Earth Systems Technology,
University of Maryland, Baltimore County, Baltimore, Maryland

(Manuscript received 18 November 2005, in final form 13 July 2006)

ABSTRACT

The 3D Goddard Cumulus Ensemble model is used to simulate two convective events observed during the Tropical Rainfall Measuring Mission Large-Scale Biosphere–Atmosphere (TRMM LBA) experiment in Brazil. These two events epitomized the type of convective systems that formed in two distinctly different environments observed during TRMM LBA. The 26 January 1999 squall line formed within a sheared low-level easterly wind flow. On 23 February 1999, convection developed in weak low-level westerly flow, resulting in weakly organized, less intense convection. Initial simulations captured the basic organization and intensity of each event. However, improvements to the model resolution and microphysics produced better simulations as compared to observations. More realistic diurnal convective growth was achieved by lowering the horizontal grid spacing from 1000 to 250 m. This produced a gradual transition from shallow to deep convection that occurred over a span of hours as opposed to an abrupt appearance of deep convection. Eliminating the dry growth of graupel in the bulk microphysics scheme effectively removed the unrealistic presence of high-density ice in the simulated anvil. However, comparisons with radar reflectivity data using contoured-frequency-with-altitude diagrams (CFADs) revealed that the resulting snow contents were too large. The excessive snow was reduced primarily by lowering the collection efficiency of cloud water by snow and resulted in further agreement with the radar observations. The transfer of cloud-sized particles to precipitation-sized ice appears to be too efficient in the original scheme. Overall, these changes to the microphysics lead to more realistic precipitation ice contents in the model. However, artifacts due to the inability of the one-moment scheme to allow for size sorting, such as excessive low-level rain evaporation, were also found but could not be resolved without moving to a two-moment or bin scheme. As a result, model rainfall histograms underestimated the occurrence of high rain rates compared to radar-based histograms. Nevertheless, the improved precipitation-sized ice signature in the model simulations should lead to better latent heating retrievals as a result of both better convective–stratiform separation within the model as well as more physically realistic hydrometeor structures for radiance calculations.

1. Introduction

Cloud models serve as a valuable tool for inferring information about clouds that cannot be directly measured such as latent heating (Tao et al. 1990, 1993b, 2000, 2001; Olson et al. 1999; Yang and Smith 1999a,b, 2000; Shige et al. 2004), budget sensitivities (Tao et al. 1993a), cloud–radiation interaction (Tao et al. 1996),

and remote sensing of precipitation (Szejwach et al. 1986; Mugnai et al. 1990, 1993; Adler et al. 1991; Smith et al. 1992, 1994; Kummerow et al. 1996; Panegrossi et al. 1998; Olson et al. 2006). Furthermore, these models provide a means to improve deficiencies in larger-scale models. A central objective of the Global Energy and Water-Cycle Experiment (GEWEX) Cloud System Study (GCSS) is to improve the parameterization of cloud systems in large-scale models by improving our understanding of cloud system processes using cloud-resolving models (CRMs; Moncrieff et al. 1997). It is imperative therefore that CRM results are carefully verified with observational data to ensure that the in-

Corresponding author address: Mr. Stephen Lang, Mesoscale Atmospheric Processes Branch, Code 613.1, NASA Goddard Space Flight Center, Greenbelt, MD 20771.
E-mail: lang@agnes.gsfc.nasa.gov

DOI: 10.1175/JAS3879.1

© 2007 American Meteorological Society



Airborne validation of spatial properties measured by the CALIPSO lidar

Matthew J. McGill,¹ Mark A. Vaughan,² Charles R. Trepte,³ William D. Hart,⁴ Dennis L. Hlavka,⁴ David M. Winker,³ and Ralph Kuehn²

Received 9 April 2007; revised 24 June 2007; accepted 16 July 2007; published 17 October 2007.

[1] The Cloud-Aerosol Lidar Infrared Pathfinder Satellite Observations (CALIPSO) satellite provides a new and exciting opportunity to study clouds and aerosols in the Earth's atmosphere using range-resolved laser remote sensing. Following the successful launch of the CALIPSO satellite, validation flights were conducted using the long-established Cloud Physics Lidar (CPL) to verify CALIPSO's calibration and validate various CALIPSO data products. This paper presents results of the initial comparisons made between the spaceborne CALIPSO lidar and the airborne CPL. Results are presented to validate measurement sensitivity and the spatial properties reported in the CALIPSO data products. Cloud layer top determinations from CALIPSO are found to be in good agreement with those from CPL. Determinations of minimum detectable backscatter are in excellent agreement with theoretical values predicted prior to launch.

Citation: McGill, M. J., M. A. Vaughan, C. R. Trepte, W. D. Hart, D. L. Hlavka, D. M. Winker, and R. Kuehn (2007), Airborne validation of spatial properties measured by the CALIPSO lidar, *J. Geophys. Res.*, 112, D20201, doi:10.1029/2007JD008768.

1. Introduction

[2] The successful launch of the Cloud-Aerosol Lidar Infrared Pathfinder Satellite Observations (CALIPSO) satellite in April 2006 ushered in a new era in satellite-based remote sensing [Winker *et al.*, 2003, 2007]. The primary payload aboard CALIPSO is the Cloud-Aerosol Lidar with Orthogonal Polarization (CALIOP), a dual wavelength, polarization-sensitive backscatter lidar that measures vertical profiles of the spatial and optical characteristics of clouds and aerosols in the Earth's atmosphere.

[3] The CALIPSO satellite is an important component of NASA's "A-train" constellation, which is a group of five formation-flying remote sensing satellites. The instruments in the A-Train were chosen to provide a comprehensive suite of measurements, both passive and active, to enable improved understanding of the Earth's atmosphere. The A-Train is named for the Aqua satellite [Parkinson, 2003] which leads the procession. Closely following Aqua are the CloudSat [Stephens *et al.*, 2002], CALIPSO, PARASOL [Steinmetz *et al.*, 2005], and Aura [Schoeberl *et al.*, 2006] satellites. The A-Train satellites fly in a 705-km Sun-synchronous orbit with a 1330 local time equatorial crossing time. With the simultaneous addition of CALIPSO and CloudSat, A-Train researchers will for the first time have access to a global suite of collocated vertical profile

measurements to augment the horizontal plane data acquired by existing passive sensors.

[4] The CALIPSO satellite became operational on 7 June 2006. While CALIPSO data will be a valuable source of research data, it is important that the CALIPSO measurements be validated so that the research community can use CALIPSO data with confidence. Accordingly, after initial data verification, aircraft flights were conducted to verify CALIPSO calibration and to validate the level 1 data products.

2. CALIPSO-CloudSat Validation Experiment (CC-VEX)

[5] During the period 26 July to 14 August 2006, the ER-2 Cloud Physics Lidar (CPL) [McGill *et al.*, 2002, 2003] was used for validation of the CALIPSO satellite lidar. The CPL provides high-resolution profiling of clouds and aerosol layers for use in cloud and radiation studies. The CPL is a state-of-the-art system operating at 1064 nm, 532 nm, and 355 nm, with linear depolarization measured using the 1064 nm channel. Measuring the backscattered signal at multiple wavelengths provides information about cloud and aerosol optical properties and the depolarization measurement can be used to determine the ice-water phase of clouds. The CPL provides data products similar to those of the CALIPSO satellite lidar and as such is an excellent CALIPSO simulator and validation tool.

[6] The high-altitude NASA ER-2 aircraft was used for the validation flights owing to its ability to fly above 20 km altitude and thereby provide "satellite-like" measurements. The flights were meant to simultaneously validate multiple aspects of the NASA A-Train of satellites, including the CloudSat radar. The payload for the CC-VEX mission included the CPL, the Cloud Radar System (CRS) [Li *et*

¹NASA Goddard Space Flight Center, Greenbelt, Maryland, USA.

²Science Systems and Applications, Inc., Hampton, Virginia, USA.

³NASA Langley Research Center, Hampton, Virginia, USA.

⁴Science Systems and Applications, Inc., Greenbelt, Maryland, USA.

Cloud Resolving Modeling

Wei-Kuo TAO

Laboratory for Atmospheres, NASA Goddard Space Flight Center, Greenbelt, Maryland, U.S.A.

(Manuscript received 12 October 2006, in final form 12 February 2007)

Abstract

One of the most promising methods to test the representation of cloud processes used in climate models is to use observations together with cloud resolving models (CRMs). CRMs use more sophisticated and realistic representations of cloud microphysical processes, and they can reasonably well resolve the time evolution, structure, and life cycles of clouds and cloud systems (with sizes ranging from about 2–200 km). CRMs also allow for explicit interaction between clouds, outgoing longwave (cooling) and incoming solar (heating) radiation, and ocean and land surface processes. Observations are required to initialize CRMs and to validate their results.

This paper provides a brief discussion and review of the main characteristics of CRMs as well as some of their major applications. These include the use of CRMs to improve our understanding of: (1) convective organization, (2) cloud temperature and water vapor budgets, and convective momentum transport, (3) diurnal variation of precipitation processes, (4) radiative-convective quasi-equilibrium states, (5) cloud-chemistry interaction, (6) aerosol-precipitation interaction, and (7) improving moist processes in large-scale models. In addition, current and future developments and applications of CRMs will be presented.

1. Introduction

Understanding the hydrological cycle is crucial in climate modeling and climate change. The hydrological cycle distinguishes the Earth from the other planets. A key link in the hydrological cycle is the rain that falls from clouds and cloud systems in the Tropics, which amounts to about two-thirds of the global precipitation. The vertical distribution of latent heat release by these clouds/convective systems can also modulate the large-scale tropical circulation (Hartmann et al. 1984; Sui and Lau 1989; and others), which, in turn, impacts midlatitude weather through teleconnection patterns such as those associated with El Niño. Furthermore, changes in the moisture distribution at

middle and upper levels of the troposphere as well as the radiative responses of cloud hydrometeors to outgoing longwave and incoming shortwave radiation are a major factor in determining whether the earth system will warm or cool as the cloud systems respond to changes in their environment (Ramanathan and Collins 1991; Lindzen 1990a, b; Betts 1990; Lau et al. 1993).

Cloud resolving models have been used to improve our understanding of cloud and precipitation processes and phenomena from micro-scale to cloud-scale and mesoscale as well as their interactions with radiation and surface processes. For example, cloud models have been used to study the mechanisms associated with cloud-cloud interactions and mergers (see Tao 2003 for a review), ice processes and their role in stratiform rain formation and their effect on cloud system mass, temperature and water vapor budgets (see Tao and Moncrieff 2003 for a review), precipitation efficiency (see Tao et

Corresponding author: Wei-Kuo Tao, Code 613.1, NASA Goddard Space Flight Center, Greenbelt, MD 20771, USA.
E-mail: tao@agnes.gsfc.nasa.gov
© 2007, Meteorological Society of Japan



Role of atmospheric aerosol concentration on deep convective precipitation: Cloud-resolving model simulations

Wei-Kuo Tao,¹ Xiaowen Li,^{1,2} Alexander Khain,³ Toshihisa Matsui,^{1,2} Stephen Lang,⁴ and Joanne Simpson¹

Received 30 March 2007; revised 28 September 2007; accepted 22 October 2007; published 22 December 2007.

[1] A two-dimensional cloud-resolving model with detailed spectral bin microphysics is used to examine the effect of aerosols on three different deep convective cloud systems that developed in different geographic locations: south Florida, Oklahoma, and the central Pacific. A pair of model simulations, one with an idealized low cloud condensation nuclei (CCN) (clean) and one with an idealized high CCN (dirty environment), is conducted for each case. In all three cases, rain reaches the ground earlier for the low-CCN case. Rain suppression is also evident in all three cases with high CCN. However, this suppression only occurs during the early stages of the simulations. During the mature stages of the simulations the effects of increasing aerosol concentration range from rain suppression in the Oklahoma case to almost no effect in the Florida case to rain enhancement in the Pacific case. The model results suggest that evaporative cooling in the lower troposphere is a key process in determining whether high CCN reduces or enhances precipitation. Stronger evaporative cooling can produce a stronger cold pool and thus stronger low-level convergence through interactions with the low-level wind shear. Consequently, precipitation processes can be more vigorous. For example, the evaporative cooling is more than two times stronger in the lower troposphere with high CCN for the Pacific case. Sensitivity tests also suggest that ice processes are crucial for suppressing precipitation in the Oklahoma case with high CCN. A comparison and review of other modeling studies are also presented.

Citation: Tao, W.-K., X. Li, A. Khain, T. Matsui, S. Lang, and J. Simpson (2007), Role of atmospheric aerosol concentration on deep convective precipitation: Cloud-resolving model simulations, *J. Geophys. Res.*, *112*, D24S18, doi:10.1029/2007JD008728.

1. Introduction

[2] Aerosols and especially their effect on clouds are one of the key components of the climate system and the hydrological cycle [Ramanathan *et al.*, 2001]. Yet, the aerosol effect on clouds remains largely unknown and the processes involved not well understood. A recent report published by the National Academy of Science states “The greatest uncertainty about the aerosol climate forcing—indeed, the largest of all the uncertainties about global climate forcing—is probably the indirect effect of aerosols on clouds” [National Research Council, 2005, p. 29]. The aerosol effect on clouds is often categorized into the traditional “first indirect (i.e., Twomey)” effect on the cloud droplet sizes for a constant liquid water

path [Twomey, 1977] and the “semidirect” effect on cloud coverage [e.g., Ackerman *et al.*, 2000]. Enhanced aerosol concentrations can also suppress warm rain processes by producing a narrow droplet spectrum that inhibits collision and coalescence processes [e.g., Squires and Twomey, 1960; Warner and Twomey, 1967; Warner, 1968; Rosenfeld, 1999].

[3] The aerosol effect on precipitation processes, also known as the second type of aerosol indirect effect [Albrecht, 1989], is even more complex, especially for mixed-phase convective clouds. A combination of cloud top temperature and effective droplet sizes, estimated from the Advanced Very High Resolution Radiometer (AVHRR), has been used to infer the suppression of coalescence and precipitation processes for smoke [Rosenfeld and Lensky, 1998] and desert dust [Rosenfeld *et al.*, 2001]. Multisensor (passive/active microwave and visible and infrared sensors) satellite observations from the Tropical Rainfall Measuring Mission (TRMM) have been used to infer the presence of nonprecipitating supercooled liquid water near the cloud top due to overseeding from both smoke over Indonesia [Rosenfeld, 1999] and urban pollution over Australia [Rosenfeld, 2000]. In addition, aircraft measurements have provided evidence of sustained supercooled liquid

¹Laboratory for Atmospheres, NASA Goddard Space Flight Center, Greenbelt, Maryland, USA.

²Goddard Earth Sciences and Technology Center, University of Maryland, Baltimore County, Baltimore, Maryland, USA.

³Department of Atmospheric Science, Hebrew University of Jerusalem, Jerusalem, Israel.

⁴Science Systems and Applications, Inc., Lanham, Maryland, USA.



Properties of light stratiform rain derived from 10- and 94-GHz airborne Doppler radars measurements

Lin Tian,^{1,2} Gerald M. Heymsfield,² Lihua Li,^{1,2} and Ramesh C. Srivastava³

Received 12 October 2006; revised 12 January 2007; accepted 16 February 2007; published 12 June 2007.

[1] This paper presents an initial investigation of using airborne Doppler radar operating at 10 and 94 GHz to measure the light stratiform rain ($\leq 5 \text{ mm hr}^{-1}$). It has been shown that the combination of 10 and 94 GHz is more sensitive to resolve the raindrop size distribution (RSD) in light rain than that of 14 and 35 GHz. A case of light stratiform rain over southern Florida is examined in detail in this study. Techniques for retrieving the profiles of a Gamma raindrop size distribution (RSD), vertical air velocity, and attenuation by precipitation and water vapor are presented. This approach uses the difference of the Doppler velocity at two frequencies and yields both RSD and the vertical air motion. The approach is primarily applicable to rain rates less than 5 mm hr^{-1} . The magnitudes of the retrieved RSD are similar to those found in ground-based observations of light stratiform rain. The retrieved vertical winds with downdrafts below about 3 km and weak updraft above are similar to what has been observed in widespread stratiform rain with melting band. The sensitivities of the retrieval to Gamma shape parameter are discussed.

Citation: Tian, L., G. M. Heymsfield, L. Li, and R. C. Srivastava (2007), Properties of light stratiform rain derived from 10- and 94-GHz airborne Doppler radars measurements, *J. Geophys. Res.*, 112, D11211, doi:10.1029/2006JD008144.

1. Introduction

[2] The vertical profiles of raindrop size distribution (RSD), vertical air velocity, precipitation, and water vapor distribution are important for studying the latent heating/cooling profile of precipitation yet are difficult to measure. Over the past several years, the Tropical Rainfall Measuring Mission (TRMM) [Kummerow *et al.*, 2000] has provided data for improving weather prediction and understanding precipitation structure and formation. Measurements by the single-wavelength TRMM precipitation radar (PR) have been used to estimate attenuation-corrected reflectivity and, from that, the rainfall rate [Iguchi *et al.*, 2000]. The data have also been used in conjunction with numerical cloud models to estimate latent heating/cooling [Tao *et al.*, 2000].

[3] One of the main uncertainties in estimating rainfall rate from the TRMM single-wavelength PR is the variability in the raindrop size distribution (RSD). A dual-wavelength radar, with a carefully selected frequency pair, can help to reduce this uncertainty. The upcoming Global Precipitation Measurement (GPM) dual-frequency radar (14 and 35 GHz) can provide RSD information and hence improve the accuracy of rainfall estimation. Many dual-frequency rain-profiling algorithms have been proposed to

date, starting with those developed by Eccles and Muller [1971], Fujita [1983], Meneghini *et al.* [1992], and Marzoug and Amayenc [1994]. These approaches start by assuming a two-parameter analytic RSD and proceed to develop a procedure to retrieve the parameters given the reflectivity profiles at the two frequencies. Doppler velocities are not considered in those approaches. At vertical incidence, the Doppler velocity is essentially due to the vertical air velocity and the fall velocity of the scattering particles. A number of investigators have shown that, under certain assumptions, the vertical air velocity and raindrop size distribution can be deduced from the mean Doppler velocity and reflectivity [e.g., Atlas and Matejka, 1985; Ulbrich, 1991]. Basic limitations of these methods are the errors incurred because of errors in deduced vertical winds and the effect of the turbulence. Meneghini *et al.* [2003] has explored the possibility of using the difference of Doppler velocities at 13.6 and 35 GHz, which is not affected by the vertical air motion, to improve the RSD estimation.

[4] In this study, we use a dual-frequency Doppler radar system operating at 10 and 94 GHz. In light rain, this system may resolve the RSD better than the GPM frequency pair because the difference in reflectivities at 14 and 35 GHz is small [Haddad *et al.*, 2006] compared to that at 10 and 94 GHz. Moreover, Doppler velocities measured by our system help to further resolve the RSD at vertical incidence. A disadvantage of the 94-GHz frequency is that it suffers greater attenuation than the GPM frequencies. This limits the 94 GHz system to light rain of intensity $\leq 5 \text{ mm hr}^{-1}$, but it would be capable of detecting much lighter rain (and high level ice clouds) than either the GPM or the TRMM radars. Moreover, light rain may have a greater impact on

¹Goddard Earth Science and Technology Center, University of Maryland, Baltimore County, Maryland, USA.

²NASA Goddard Space Flight Center, Greenbelt, Maryland, USA.

³Department of the Geophysical Sciences, The University of Chicago, Chicago, Illinois, USA.

Cloud Optical Depth Retrievals From Solar Background “Signals” of Micropulse Lidars

J. Christine Chiu, Alexander Marshak, Warren J. Wiscombe, Sandra C. Valencia, and E. Judd Welton

Abstract—Pulsed lidars are commonly used to retrieve vertical distributions of cloud and aerosol layers. It is widely believed that lidar cloud retrievals (other than cloud base altitude) are limited to optically thin clouds. Here, we demonstrate that lidars can retrieve optical depths of thick clouds using solar background light as a signal, rather than (as now) merely a noise to be subtracted. Validations against other instruments show that retrieved cloud optical depths agree within 10%–15% for overcast stratus and broken clouds. In fact, for broken cloud situations, one can retrieve not only the aerosol properties in clear-sky periods using lidar signals, but also the optical depth of thick clouds in cloudy periods using solar background signals. This indicates that, in general, it may be possible to retrieve both aerosol and cloud properties using a single lidar. Thus, lidar observations have great untapped potential to study interactions between clouds and aerosols.

Index Terms—Cloud, cloud–aerosol interactions, lidar, remote sensing, zenith radiance.

I. INTRODUCTION

MICROPULSE lidar (MPLs) systems, developed in 1992 [1], are now widely used to retrieve heights of cloud layers and vertical distributions of aerosols layers [2], [3]. The MPL time-dependent returned signal is proportional to the amount of light backscattered by atmospheric molecules, aerosols, and clouds. However, measured photon counts must be converted to attenuated backscatter profiles, and during the process a number of noise sources need to be accounted for [4] and [5].

One source of noise is solar background light, which is measured by the MPL detector in addition to backscattered laser light. The MPL has a narrow field of view and filter bandwidth to reduce solar noise, but the contribution remains significant near solar noon or when a bright cloud is overhead. Fortunately, this noise can be estimated. Due to a time interval of 400 μ s between consecutive pulses, data can be retrieved up to a range of 60 km. However, there is no discernible

backscatter beyond 30 km. Therefore, we can estimate solar background light using sample bins between 45 and 55 km.

One man’s noise is another man’s signal. When lidars point straight up, the solar background noise is the solar zenith radiance, which can be used to retrieve cloud optical properties [6], [7]. We are unaware of any retrieval algorithm that uses the solar background light observed by lidars as a signal. This letter aims to address this issue by providing a proof-of-concept for using solar background “signal” from MPL to retrieve cloud optical depth. We will also evaluate results against those retrieved from other methods, and discuss the potential of our method to shed light on aerosol–cloud interactions.

II. APPROACH

Solar background signal is estimated from lidar bins beyond 30 km in units of photon counts. For retrieval purposes, photon counts must be converted to actual radiance. This conversion is instrument-dependent. [8] described a laboratory calibration procedure capable of converting raw detector counts to calibrated radiance. The authors demonstrated that the calibrated MPL solar background radiance agreed with zenith radiance measurements from principal plane observations using a collocated AERONET sunphotometer [9]. Thus, it is possible to calibrate MPL systems using the collocated AERONET sunphotometers instead of the more time-consuming laboratory calibration. The sunphotometer calibration method would also account for MPL calibration drifts during the period of MPL deployment (due to filter degradation and window cleanliness). In this letter, we followed their method and derived MPL calibration coefficients using AERONET data when available.

MPLs of the atmospheric radiation measurement (ARM) program and of the NASA MPL Network (MPLNET [10]) both operate at a 523-nm wavelength. The general relationship between zenith radiance and cloud optical depth at this wavelength is depicted in Fig. 1, based on 1-D plane-parallel radiative transfer. Clearly, this relationship is not a one-to-one function. There are two cloud optical depths that give the same zenith radiance: one corresponds to thinner clouds and the other to thicker clouds. Thus, it is impossible to unambiguously retrieve cloud optical depth from solar background signal of a one-channel MPL. To remove this ambiguity, a criterion is needed to distinguish thick clouds from thin clouds or no clouds. A simple criterion adapted here assumes that if a lidar beam is completely attenuated, the detected clouds correspond to the larger optical depth.

Retrievals from MPL solar background signal are intercompared with those from three other instruments. The first instrument is the ARM multifilter rotating shadowband radiometer

Manuscript received July 25, 2006; revised December 11, 2006. This work was supported by the Office of Science (BER), U.S. Department of Energy under Grant DE-AI02-95ER61961, as part of the ARM program. The NASA Earth Observing System and Radiation Sciences Program supported MPLNET.

J. C. Chiu is with the Joint Center for Earth Systems Technology, University of Maryland Baltimore County, Baltimore, MD 21250 USA (e-mail: cchiu@climate.gsfc.nasa.gov).

A. Marshak, W. J. Wiscombe, and E. J. Welton are with the NASA Goddard Space Flight Center, Greenbelt, MD 20771 USA (e-mail: Alexander.Marshak@nasa.gov; Warren.J.Wiscombe@nasa.gov; Ellsworth.J.Welton@nasa.gov).

S. C. Valencia was with Science, Systems, and Applications, Inc., Lanham, MD 20706 USA, and the NASA Goddard Space Flight Center, Greenbelt, MD 20771 USA. She is now with the London School of Economics and Political Science, WC2A 2AE London, U.K. (e-mail: s.c.valencia@lse.ac.uk).

Digital Object Identifier 10.1109/LGRS.2007.896722

U.S. Government work not protected by U.S. copyright.



Satellite-derived aerosol optical depth over dark water from MISR and MODIS: Comparisons with AERONET and implications for climatological studies

Ralph A. Kahn,¹ Michael J. Garay,¹ David L. Nelson,¹ Kevin K. Yau,¹ Michael A. Bull,¹ Barbara J. Gaitley,¹ John V. Martonchik,¹ and Robert C. Levy²

Received 23 October 2006; revised 30 March 2007; accepted 26 June 2007; published 26 September 2007.

[1] Although the current Multiangle Imaging Spectroradiometer (MISR) and Moderate Resolution Imaging Spectroradiometer (MODIS) satellite passive remote sensing midvisible aerosol optical thickness (AOT) products are accurate overall to about 0.05 or 20%, they differ systematically on a global, monthly average basis, by about 0.03 to 0.05. Some key climate change and other applications require accuracies of 0.03 or better. The instruments are sufficiently stable and well characterized, and have adequate signal-to-noise, to realize such precision. However, assumptions made in the current standard aerosol retrieval algorithms produce AOT biases that must be addressed first. We identify the causes of AOT discrepancies over dark water under typical, relatively low AOT conditions and quantify their magnitudes on the basis of detailed analysis. Examples were selected to highlight key issues for which there are coincident MISR, MODIS, and Aerosol Robotic Network (AERONET) observations. Instrument calibration and sampling differences, assumptions made in the MISR and MODIS standard algorithms about ocean surface boundary conditions, missing particle property or mixture options, and the way reflectances used in the retrievals are selected each contribute significantly to the observed differences under some circumstances. Cloud screening is also identified as a factor, though not fully examined here, as are the relatively rare high-AOT cases over ocean. Specific algorithm upgrades and further studies indicated by these findings are discussed, along with recommendations for effectively using the currently available products for regional and global applications.

Citation: Kahn, R. A., M. J. Garay, D. L. Nelson, K. K. Yau, M. A. Bull, B. J. Gaitley, J. V. Martonchik, and R. C. Levy (2007), Satellite-derived aerosol optical depth over dark water from MISR and MODIS: Comparisons with AERONET and implications for climatological studies, *J. Geophys. Res.*, *112*, D18205, doi:10.1029/2006JD008175.

1. Introduction

[2] The Multiangle Imaging Spectroradiometer (MISR) [Diner *et al.*, 1998] began taking data in late February 2000. Since then, numerous studies have compared aerosol optical thickness (AOT) retrieved from the instrument's 36 spectral angular channels with similar quantities derived from the Aerosol Robotic Network (AERONET) [Holben *et al.*, 1998] Sun photometer network, the Moderate Resolution Imaging Spectroradiometer (MODIS) [Barnes *et al.*, 1998; Salomonson *et al.*, 1989] that flies aboard the Terra satellite with MISR, and other regional and global observations [e.g., Abdou *et al.*, 2005; Christopher and Wang, 2004; Diner *et al.*, 2001; Kahn *et al.*, 2005a, 2005b; Liu *et al.*, 2004; Martonchik *et al.*, 2004; Myhre *et al.*, 2005; Redemann *et al.*, 2005; Schmid *et al.*, 2003; Yu *et al.*, 2006].

That work demonstrates the MISR Standard Aerosol Retrieval algorithm (V16 or lower) retrieves AOT over land and water, with overall statistical accuracy better than 0.05 or 20%, whichever is larger, and with greater accuracy over some surfaces such as dark water. Similar results are reported for MODIS-AERONET AOT comparisons [Remer *et al.*, 2005; Levy *et al.*, 2003, 2005; Chu *et al.*, 2002; L. A. Remer *et al.*, 2006, Algorithm for remote sensing of tropospheric aerosol from MODIS: Collection 5, available at http://modis-atmos.gsfc.nasa.gov/reference_atbd.php; hereinafter referred to as Remer *et al.*, 2006].

[3] However, some blunders occur, often because of inadequate cloud screening or inaccurate surface property assumptions, and persistent small but systematic differences between MISR and MODIS AOT values can be significant when large aggregates of measurements from the two instruments are compared. MODIS produces generally higher midvisible AOT than MISR and AERONET over land, whereas MISR AOT is generally higher than MODIS over water [e.g., Abdou *et al.*, 2005; Myhre *et al.*, 2005]. Recent improvements in MISR band-to-band and camera-to-camera calibration have reduced average MISR-

¹Jet Propulsion Laboratory, California Institute of Technology, Pasadena, California, USA.

²NASA Goddard Space Flight Center, Greenbelt, Maryland, USA.

Atmos. Chem. Phys. Discuss., 7, 4481–4519, 2007
www.atmos-chem-phys-discuss.net/7/4481/2007/
© Author(s) 2007. This work is licensed
under a Creative Commons License.



Remote sensing the vertical profile of cloud droplet effective radius, thermodynamic phase, and temperature

J. Vanderlei Martins^{1,2}, A. Marshak², L. A. Remer², D. Rosenfeld³,
Y. J. Kaufman², R. Fernandez-Borda⁴, I. Koren⁵, V. Zubko⁶, and P. Artaxo⁷

¹Department of Physics, and Joint Center for Earth Systems Technology, University of Maryland Baltimore County, Baltimore, MD, USA

²Climate and Radiation Branch, NASA – Goddard Space Flight Center, Greenbelt, MD, USA

³Institute of Earth Sciences, The Hebrew University of Jerusalem, Israel

⁴Catholic University, Washington DC, USA

⁵Department of Environmental Sciences, Weizmann Institute, Rehovot, Israel

⁶Advanced Computation Technologies, Inc., Lanham, MD, USA

⁷Institute of Physics, University of Sao Paulo, Brazil

Received: 7 November 2006 – Accepted: 30 January 2007 – Published: 30 March 2007

Correspondence to: J. Vanderlei Martins (martins@climate.gsfc.nasa.gov)

4481

Abstract

Cloud-aerosol interaction is no longer simply a radiative problem, but one affecting the water cycle, the weather, and the total energy balance including the spatial and temporal distribution of latent heat release. Information on the vertical distribution of cloud droplet microphysics and thermodynamic phase as a function of temperature or height, can be correlated with details of the aerosol field to provide insight on how these particles are affecting cloud properties and its consequences to cloud lifetime, precipitation, water cycle, and general energy balance. Unfortunately, today's experimental methods still lack the observational tools that can characterize the true evolution of the cloud microphysical, spatial and temporal structure in the cloud droplet scale, and then link these characteristics to environmental factors and properties of the cloud condensation nuclei.

Here we propose and demonstrate a new experimental approach (the cloud scanner instrument) that provides the microphysical information missed in current experiments and remote sensing options. Cloud scanner measurements can be performed from aircraft, ground, or satellite by scanning the side of the clouds from the base to the top, providing us with the unique opportunity of obtaining snapshots of the cloud droplet microphysical and thermodynamic states as a function of height and brightness temperature in clouds at several development stages. The brightness temperature profile of the cloud side can be directly associated with the thermodynamic phase of the droplets to provide information on the glaciation temperature as a function of different ambient conditions, aerosol concentration, and type. An aircraft prototype of the cloud scanner was built and flew in a field campaign in Brazil.

The CLAIM-3D (3-Dimensional Cloud Aerosol Interaction Mission) satellite concept proposed here combines several techniques to simultaneously measure the vertical profile of cloud microphysics, thermodynamic phase, brightness temperature, and aerosol amount and type in the neighborhood of the clouds. The wide wavelength range, and the use of multi-angle polarization measurements proposed for this mis-

4482

The Plane-Parallel Albedo Bias of Liquid Clouds from MODIS Observations

LAZAROS OREOPOULOS

Joint Center for Earth Systems Technology, University of Maryland, Baltimore County, Baltimore, and Laboratory for Atmospheres, NASA Goddard Space Flight Center, Greenbelt, Maryland

ROBERT F. CAHALAN AND STEVEN PLATNICK

Laboratory for Atmospheres, NASA Goddard Space Flight Center, Greenbelt, and Joint Center for Earth Systems Technology, University of Maryland, Baltimore County, Baltimore, Maryland

(Manuscript received 7 August 2006, in final form 12 March 2007)

ABSTRACT

The authors present the global plane-parallel shortwave albedo bias of liquid clouds for two months, July 2003 and January 2004. The cloud optical properties necessary to perform the bias calculations come from the operational Moderate Resolution Imaging Spectroradiometer (MODIS) *Terra* and MODIS *Aqua* level-3 datasets. These data, along with ancillary surface albedo and atmospheric information consistent with the MODIS retrievals, are inserted into a broadband shortwave radiative transfer model to calculate the fluxes at the atmospheric column boundaries. The plane-parallel homogeneous (PPH) calculations are based on the mean cloud properties, while independent column approximation (ICA) calculations are based either on 1D histograms of optical thickness or joint 2D histograms of optical thickness and effective radius. The (positive) PPH albedo bias is simply the difference between PPH and ICA albedo calculations. Two types of biases are therefore examined: 1) the bias due to the horizontal inhomogeneity of optical thickness alone (the effective radius is set to the grid mean value) and 2) the bias due to simultaneous variations of optical thickness and effective radius as derived from their joint histograms. The authors find that the global bias of albedo (liquid cloud portion of the grid boxes only) is $\sim +0.03$, which corresponds to roughly 8% of the global liquid cloud albedo and is only modestly sensitive to the inclusion of horizontal effective radius variability and time of day, but depends strongly on season and latitude. This albedo bias translates to ~ -3 – -3.5 W m^{-2} of bias (stronger negative values) in the diurnally averaged global shortwave cloud radiative forcing, assuming homogeneous conditions for the fraction of the grid box not covered by liquid clouds; zonal values can be as high as 8 W m^{-2} . Finally, the (positive) broadband atmospheric absorptance bias is about an order of magnitude smaller than the albedo bias. The substantial magnitude of the PPH bias underlines the importance of predicting subgrid variability in GCMs and accounting for its effects on cloud–radiation interactions.

1. Introduction

The bias in solar radiative fluxes within a model or other large-scale grid due to the assumption of horizontal homogeneity in cloud optical thickness τ [plane-parallel homogeneous (PPH) bias] received a great amount of attention following the publication of the study by Cahalan et al. (1994), but its existence and potential importance had already emerged in earlier publications (Harshvardhan and Randall 1985; Stephens 1988). Cahalan et al. provided a theoretical framework

for studying the PPH bias by using a fractal cloud model but restricted the quantitative analysis of cloud inhomogeneity on marine stratocumulus clouds with properties derived from surface microwave radiometer observations. Cloud microphysics (i.e., droplet effective radius r_e) was assumed constant ($r_e = 10$ μm), surface and atmospheric effects were neglected, and the radiative transfer did not extend beyond monochromatic calculations. For typical marine stratocumulus observed during the First International Satellite Cloud Climatology Project (ISCCP) Regional Experiment (FIRE), Cahalan et al. found a value of $\sim +0.09$ as representative of the PPH albedo bias at visible wavelengths. Subsequent observationally based work (Barker 1996; Oreopoulos and Davies 1998; Pincus et al. 1999; Ros-

Corresponding author address: Lazaros Oreopoulos, NASA Goddard Space Flight Center, Code 613.2, Greenbelt, MD 20771.
E-mail: lazarus@climate.gsfc.nasa.gov



Potential for airborne offbeam lidar measurements of snow and sea ice thickness

Tamás Várnai¹ and Robert F. Cahalan²

Received 4 January 2007; revised 23 June 2007; accepted 17 August 2007; published 14 December 2007.

[1] This article discusses the capabilities and limitations of a new approach to airborne measurements of snow and sea ice thickness. Such measurements can help better understand snow and sea ice processes and can also contribute to the validation of satellite measurements. The approach discussed here determines physical snow and sea ice thickness by observing the horizontal spread of lidar pulses: The bright halo observed around an illuminated spot extends farther out in thicker layers because photons can travel longer without escaping through the bottom. Since earlier studies suggested the possibility of such sea ice retrievals, this article presents a theoretical analysis of additional uncertainties that arise in airborne observations of snow and sea ice. Snow and sea ice retrievals pose somewhat different challenges because while sea ice is usually much thicker, snow contains a much higher concentration of scatterers. As a result, sea ice halos are larger, but snow halos are brighter. The results indicate that airborne sea ice retrievals are possible at night and that snow retrievals are possible during both night and day. For snow thicknesses less than about 50 cm, observational issues, such as calibration uncertainty, can cause retrieval uncertainties on the order of 10% in 1-km-resolution retrievals. For moderate snow and sea ice thicknesses (<30 cm and 3 m, respectively), these issues cause similar (~10%) uncertainties in sea ice thickness retrievals as well. These results indicate that offbeam lidars have the potential to become an important component of future snow and sea ice observing systems.

Citation: Várnai, T., and R. F. Cahalan (2007), Potential for airborne offbeam lidar measurements of snow and sea ice thickness, *J. Geophys. Res.*, 112, C12S90, doi:10.1029/2007JC004091.

1. Introduction

[2] Snow and sea ice thicknesses are not only indicators of the growth and melt of snow cover and sea ice, but they also influence surface fluxes of heat, radiation, and momentum. Yet, snow and sea ice thicknesses are among the least known parameters of the cryosphere. The pressing need for large-scale measurements of these parameters spurred the development of a variety of remote sensing methods. For example, sea ice thickness is often estimated using freeboard altimetry based on lidar or radar observations [e.g., Comiso *et al.*, 1991; Wadhams *et al.*, 1991; Laxon *et al.*, 2003] or using ice classification based on synthetic aperture radar (SAR) data [e.g., Steffen and Heinrichs, 2001; Kwok and Cunningham, 2002], whereas snow thickness is often estimated from passive microwave observations [e.g., Markus and Cavalieri, 1998; Kelly *et al.*, 2003]. These measurements provided numerous important insights but remain affected by substantial uncertainties. For example, freeboard sea ice measurements suffer from the lack of

direct information on snow thickness and from uncertainties in sea level and instrument altitude, whereas microwave snow measurements are affected by calibration uncertainties and surface roughness [e.g., Kwok *et al.*, 2004; Powell *et al.*, 2006; Stroeve *et al.*, 2006]. This article examines the feasibility of a new approach that uses offbeam lidar data for simultaneous measurements of snow and sea ice thickness.

[3] As illustrated in Figure 1, offbeam lidars detect diffuse return signals from several annular rings. These instruments determine the thickness of highly opaque media by observing the horizontal spread of lidar pulses: The bright halo observed around the illuminated spot extends farther out in thicker layers, because photons can travel farther without escaping through the bottom [e.g., Voss and Schoonmaker, 1992; Davis *et al.*, 1997; Davis and Marshak, 2002] (Figure 2). This measurement approach was used in several disciplines, providing thickness measurements for media as diverse as tooth enamel and thick clouds [e.g., Groenhius *et al.*, 1983; Cahalan *et al.*, 2005a; Polonsky *et al.*, 2005]. Moreover, results from ground-based experiments of Haines *et al.* [1997, Table 1] suggest to us that this approach can provide accurate thickness measurements for sea ice as well. (In these ground-based experiments ice thickness and extinction coefficient were obtained using data from a light detector that moved around a lamp illuminating the ice at a single point.) This article examines

¹Joint Center for Earth System Technology, University of Maryland, Baltimore County, Baltimore, Maryland, USA.

²Laboratory for Atmospheres, NASA Goddard Space Flight Center, Greenbelt, Maryland, USA.



3-D aerosol-cloud radiative interaction observed in collocated MODIS and ASTER images of cumulus cloud fields

Guoyong Wen,^{1,2} Alexander Marshak,¹ Robert F. Cahalan,¹ Lorraine A. Remer,¹ and Richard G. Kleidman³

Received 15 November 2006; revised 8 January 2007; accepted 27 March 2007; published 6 July 2007.

[1] Three-dimensional (3-D) aerosol-cloud interaction is examined by analyzing two images containing cumulus clouds in biomass-burning regions in Brazil. The research consists of two parts. The first part focuses on identifying 3-D cloud impacts on reflectances for the pixels selected for the MODIS aerosol retrieval based purely on observations. The second part of the research combines the observations with radiative transfer computations to identify key parameters in the 3-D aerosol-cloud interaction. We find that 3-D cloud-induced enhancement depends on the optical properties of nearby clouds as well as on wavelength. The enhancement is too large to be ignored. Associated bias error in one-dimensional (1-D) aerosol optical thickness retrieval ranges from 50 to 140% depending on wavelength and the optical depth of nearby clouds, as well as aerosol optical thickness. We caution the community to be prudent when applying 1-D approximations in computing solar radiation in clear regions adjacent to clouds or when using traditional retrieved aerosol optical thickness in aerosol indirect effect research.

Citation: Wen, G., A. Marshak, R. F. Cahalan, L. A. Remer, and R. G. Kleidman (2007), 3-D aerosol-cloud radiative interaction observed in collocated MODIS and ASTER images of cumulus cloud fields, *J. Geophys. Res.*, *112*, D13204, doi:10.1029/2006JD008267.

1. Introduction

[2] Aerosols play a critical role in the process of cloud formation. A change in aerosol properties may directly impact atmospheric radiation and also lead to a change in the microphysical and radiative properties of clouds and thus directly and indirectly influence the Earth's climate. Analyzing AERONET [see Holben *et al.*, 1998] ground-based network data, Kaufman and Koren [2006] recently found that absorbing and nonabsorbing aerosols affect cloud cover differently. While absorbing aerosols prevent clouds from forming, nonabsorbing aerosols extend cloud life times and are associated with enhanced cloud cover. This complements the fundamental theory of Twomey [1977] that ties an increase of anthropogenic aerosol to possible consequences to global climate change. An example of an application of this theory is the modification of cloud properties through a change in cloud condensation nuclei (CCN) in ship tracks observed from space [Platnick *et al.*, 2000; Coakley *et al.*, 1987]. However, assessing and quantifying the indirect effect of aerosol on cloud properties and climate on global scale still remains a great challenge. The

radiative forcing of aerosol indirect effect on climate has been identified as the most uncertain among other radiative forcing factors [Intergovernmental Panel on Climate Change, 2001]. For example, the effect of aerosols on cloud albedo has a large range of uncertainties estimated as cooling between -2 and 0 W/m². The level of scientific understanding of aerosol indirect effect is categorized as "very low." Global observation of aerosol and cloud properties from satellite is one way to advance our understanding of aerosol indirect effect on the Earth's climate and to reduce its uncertainties.

[3] However, aerosol and cloud properties inferred from satellite observations are subject to uncertainties. This is partly because cloud and aerosol properties are derived from the satellite-observed reflected solar radiation on the basis of various assumptions about the Earth's surface, atmosphere, aerosols, and clouds. For operational purpose, the atmosphere, aerosols, and clouds are usually assumed to be horizontally homogeneous and plane parallel, which is called the 1-D approximation or plane-parallel approximation (PPA). In this approximation, it is assumed that radiative properties of an individual pixel are independent of its neighbors. Many studies have shown that 3-D cloud structure has a complicated impact on the retrievals of cloud properties [e.g., Chambers *et al.*, 1997; Várnai and Marshak, 2002; Iwabuchi and Hayasaka, 2003; Horváth and Davies, 2004; Marshak *et al.*, 2006]. In this study, we focus on how 3-D cloud structure affects reflectance in the clear region near clouds and what are the consequences of this enhanced reflectance on aerosol retrievals.

¹NASA Goddard Space Flight Center, Greenbelt, Maryland, USA.

²Goddard Earth Sciences and Technology Center, University of Maryland Baltimore County, Baltimore County, Maryland, USA.

³Science Systems and Applications, Inc., Lanham, Maryland, USA.

The Frequency of Extreme Rain Events in Satellite Rain-Rate Estimates and an Atmospheric General Circulation Model

ERIC M. WILCOX*

Program in Atmospheric and Oceanic Sciences, Princeton University, Princeton, New Jersey

LEO J. DONNER

NOAA/Geophysical Fluid Dynamics Laboratory, Princeton University, Princeton, New Jersey

(Manuscript received 19 July 2005, in final form 2 May 2006)

ABSTRACT

The frequency distributions of surface rain rate are evaluated in the Tropical Rainfall Measuring Mission (TRMM) and Special Sensor Microwave/Imager (SSM/I) satellite observations and the NOAA/GFDL global atmosphere model version 2 (AM2). Instantaneous satellite rain-rate observations averaged over the 2.5° latitude \times 2° longitude model grid are shown to be representative of the half-hour rain rate from single time steps simulated by the model. Rain-rate events exceeding 10 mm h^{-1} are observed by satellites in most regions, with 1 mm h^{-1} events occurring more than two orders of magnitude more frequently than 10 mm h^{-1} events. A model simulation using the relaxed Arakawa-Schubert (RAS) formulation of cumulus convection exhibits a strong bias toward many more light rain events compared to the observations and far too few heavy rain events. A simulation using an alternative convection scheme, which includes an explicit representation of mesoscale circulations and an alternative formulation of the closure, exhibits, among other differences, an order of magnitude more tropical rain events above the 5 mm h^{-1} rate compared to the RAS simulation. This simulation demonstrates that global atmospheric models can be made to produce heavy rain events, in some cases even exceeding the observed frequency of such events. Additional simulations reveal that the frequency distribution of the surface rain rate in the GCM is shaped by a variety of components within the convection parameterization, including the closure, convective triggers, the spectrum of convective and mesoscale clouds, and other parameters whose physical basis is currently only understood to a limited extent. Furthermore, these components interact nonlinearly such that the sensitivity of the rain-rate distribution to the formulation of one component may depend on the formulation of the others. Two simulations using different convection parameterizations are performed using perturbed sea surface temperatures as a surrogate for greenhouse gas-forced climate warming. Changes in the frequency of rain events greater than 2 mm h^{-1} associated with changing the convection scheme in the model are greater than the changes in the frequency of heavy rain events associated with a 2-K warming using either model. Thus, uncertainty persists with respect to simulating intensity distributions for precipitation and projecting their future changes. Improving the representation of the frequency distribution of rain rates will rely on refinements in the formulation of cumulus closure and the other components of convection schemes, and greater certainty in predictions of future changes in both total rainfall and in rain-rate distributions will require additional refinements in those parameterizations that determine the cloud and water vapor feedbacks.

1. Introduction

An increase in the frequency of heavy rain events is one expected consequence of climate change associated

with increasing greenhouse gas concentrations in the atmosphere. Such a change may be expected based on simple theoretical arguments, which are now being tested in global climate model simulations of increasing greenhouse gas concentration scenarios. Many of the processes leading to precipitation, however, are not well resolved in coarse-resolution models used for global climate change prediction. As a result, the intensity of simulated rainfall events may depend strongly on the formulation of various parameterizations designed to estimate the bulk effects of subgrid-scale processes on

* Current affiliation: NASA Goddard Space Flight Center, Greenbelt, Maryland.

Corresponding author address: Eric Wilcox, NASA Goddard Space Flight Center, Code 613.2, Greenbelt, MD 20771.
E-mail: eric.m.wilcox@nasa.gov

DOI: 10.1175/JCLI3987.1

© 2007 American Meteorological Society

Use of High-Resolution Satellite Observations to Evaluate Cloud and Precipitation Statistics from Cloud-Resolving Model Simulations. Part I: South China Sea Monsoon Experiment

Y. P. ZHOU,* W.-K. TAO,⁺ A. Y. HOU,⁺ W. S. OLSON,[#] C.-L. SHIE,* K.-M. LAU,⁺ M.-D. CHOU,[@]
X. LIN,* AND M. GRECU*

*Goddard Earth Sciences and Technology Center, University of Maryland, Baltimore County, Baltimore, Maryland

⁺NASA Goddard Space Flight Center, Greenbelt, Maryland

[#]Joint Center for Earth Systems Technology, University of Maryland, Baltimore County, Baltimore, Maryland

[@]National Taiwan University, Taipei, Taiwan

(Manuscript received 25 August 2006, in final form 20 February 2007)

ABSTRACT

Cloud and precipitation simulated using the three-dimensional (3D) Goddard Cumulus Ensemble (GCE) model are compared to Tropical Rainfall Measuring Mission (TRMM) Microwave Imager (TMI) and Precipitation Radar (PR) rainfall measurements and Clouds and the Earth's Radiant Energy System (CERES) single scanner footprint (SSF) radiation and cloud retrievals. Both the model simulation and retrieved parameters are based upon observations made during the South China Sea Monsoon Experiment (SCSMEX) field campaign. The model-simulated cloud and rain systems are evaluated by systematically examining important parameters such as the surface rain rate, convective/stratiform percentage, rain profiles, cloud properties, and precipitation efficiency.

It is demonstrated that the GCE model is capable of simulating major convective system development and reproduces the total surface rainfall amount as compared to rainfall estimated from the SCSMEX sounding network. The model yields a slightly higher total convective rain/stratiform rain ratio than the TMI and PR observations. The GCE rainfall spectrum exhibits a greater contribution from heavy rains than those estimated from PR or TMI observations. In addition, the GCE simulation produces much greater amounts of snow and graupel than the TRMM retrievals. The model's precipitation efficiency of convective rain is close to the observations, but the precipitation efficiency of stratiform rain is much lower than the observations because of large amounts of slowly falling simulated snow and graupel. Compared to observations, the GCE produces more compact areas of intense convection and less anvil cloud, which are consistent with a smaller total cloud fraction and larger domain-averaged outgoing longwave radiation.

1. Introduction

Clouds and precipitation play key roles in linking the earth's energy cycle and water cycles. Clouds modulate the incoming solar radiation through reflection and the outgoing longwave radiation by altering the effective emitting temperature. Cloud itself is an important component of the hydrological cycle. Precipitation starts with cloud formation and through condensation and latent heat release it connects both the energy and water cycles. The sensitivity of deep convective cloud systems and their associated precipitation efficiency in re-

sponse to climate change are key factors in predicting the future climate.

Components of the space-based Earth Observing System (EOS), such as the National Aeronautics and Space Administration's (NASA) Clouds and the Earth's Radiant Energy System (CERES) experiment (Wielicki et al. 1996) and the Tropical Rainfall Measuring Mission (TRMM; Simpson et al. 1988, 1996) are designed to provide crucial cloud and precipitation measurements for advancing our understanding of the role of clouds and precipitation in the global energy and water cycles, and for improving their representation in general circulation and climate models. The CERES products include broadband shortwave and longwave radiation from the top of the atmosphere, as well as simultaneous cloud properties retrieved from the other

Corresponding author address: Dr. Yaping Zhou, NASA Goddard Space Flight Center, Mail Code 613.2, Greenbelt, MD 20771.
E-mail: yaping.zhou-1@nasa.gov



Sulfur dioxide emissions from Peruvian copper smelters detected by the Ozone Monitoring Instrument

S. A. Carn,¹ A. J. Krueger,¹ N. A. Krotkov,² K. Yang,² and P. F. Levelt³

Received 6 December 2006; revised 20 March 2007; accepted 5 April 2007; published 1 May 2007.

[1] We report the first daily observations of sulfur dioxide (SO₂) emissions from copper smelters by a satellite-borne sensor - the Ozone Monitoring Instrument (OMI) on NASA's EOS/Aura spacecraft. Emissions from two Peruvian smelters (La Oroya and Ilo) were detected in up to 80% of OMI overpasses between September 2004 and June 2005. SO₂ production by each smelter in this period is assessed and compared with contemporaneous emissions from active volcanoes in Ecuador and southern Colombia. Annual SO₂ discharge from the Ilo smelter, La Oroya smelter, and volcanoes in 2004–2005 is estimated and amounts to $0.3^{+0.2}_{-0.1}$, 0.07 ± 0.03 , and 1.2 ± 0.5 Tg, respectively. This study confirms OMI's potential as an effective tool for evaluation of anthropogenic and natural SO₂ emissions. Smelter plumes transport an array of toxic metals in addition to SO₂ and continued monitoring to mitigate health and environmental impacts is recommended.

Citation: Carn, S. A., A. J. Krueger, N. A. Krotkov, K. Yang, and P. F. Levelt (2007), Sulfur dioxide emissions from Peruvian copper smelters detected by the Ozone Monitoring Instrument, *Geophys. Res. Lett.*, *34*, L09801, doi:10.1029/2006GL029020.

1. Introduction

[2] Anthropogenic activities over the last century (mainly fossil fuel burning and metal smelting) have raised atmospheric SO₂ concentrations by up to 3 orders of magnitude [Pham *et al.*, 1996]. Of potentially greater significance is the concomitant increase in production of derived sulfate aerosol, which indirectly affects the climate system and water cycle by supplying cloud condensation nuclei, enhancing cloud albedo, and suppressing precipitation [Twomey, 1977; Charlson *et al.*, 1992; Rosenfeld, 2000]. An inventory of anthropogenic SO₂ source strengths is therefore a crucial component of global atmospheric models, but to date emissions from major source regions such as East Asia have typically been estimated using complex algorithms that rely on large input datasets, enumerating parameters such as fuel use and the removal efficiency of emission abatement systems [e.g., Streets *et al.*, 2003].

[3] As a viable alternative to these “bottom-up” estimates of emissions, the ultraviolet (UV) GOME and SCIAMACHY satellite sensors have demonstrated that anthropogenic SO₂ emissions can be detected from space

[e.g., Eisinger and Burrows, 1998]. However, the efficacy of GOME and SCIAMACHY data for detailed studies of SO₂ emissions is restricted by poor spatial or temporal sampling. On July 15, 2004, NASA launched the Ozone Monitoring Instrument (OMI) as part of the EOS-Aura mission (<http://aura.gsfc.nasa.gov>). OMI has a unique combination of footprint size (13×24 km at nadir), spectral resolution (0.45 nm) and global contiguous coverage for space-based UV measurements of SO₂, surpassing the sensitivity of the Earth Probe Total Ozone Mapping Spectrometer (EP-TOMS), which could only detect anthropogenic SO₂ emissions when atmospheric loadings were exceptional [Carn *et al.*, 2004]. Using algorithms developed for retrieval of SO₂ from OMI, the noise level of SO₂ measurements has been reduced by an order of magnitude compared to the TOMS instruments [Krotkov *et al.*, 2006]. As we demonstrate here, these improvements permit detection of SO₂ discharge from specific industrial sources on a daily basis.

2. OMI Instrument and SO₂ Algorithm

[4] OMI is a hyperspectral UV/Visible spectrometer with a 2600 km swath for daily, contiguous global mapping of ozone and trace gases including SO₂, NO₂ and BrO. It was contributed to the 6-year Aura mission by the Royal Netherlands Meteorological Institute (KNMI) and the Netherlands Agency for Aerospace Programs (NIVR), in collaboration with the Finnish Meteorological Institute (FMI). Operational data flow from OMI began in September 2004. The Aura spacecraft is in a sun-synchronous orbit at 705 km altitude and crosses the equator at 1:45 pm \pm 15 minutes local time each day (ascending node).

[5] Most OMI data products are currently produced using radiances at a subset of UV wavelengths calibrated with post-launch data. We have developed a scheme termed the Band Residual Difference (BRD) algorithm, which retrieves total column SO₂ using four OMI wavelengths situated at SO₂ band extrema between 310.8 and 314.4 nm [Krotkov *et al.*, 2006]. As described above, the BRD retrieval noise is an order of magnitude lower than achieved with EP-TOMS, permitting detection of weaker SO₂ sources and smaller SO₂ clouds with OMI. We have also developed time-averaging techniques which further improve the signal to noise ratio. All SO₂ data in this paper were produced using the BRD algorithm, the derivation of which is described by Krotkov *et al.* [2006].

[6] We caution that OMI SO₂ algorithms are subject to ongoing development and refinement, and that OMI SO₂ data have not yet been rigorously validated using correlative measurements. Retrieval of anthropogenic SO₂ in the planetary boundary layer (PBL) is particularly challenging due

¹Joint Center for Earth Systems Technology, University of Maryland Baltimore County, Baltimore, Maryland, USA.

²Goddard Earth Sciences and Technology Center, University of Maryland Baltimore County, Baltimore, Maryland, USA.

³Royal Netherlands Meteorological Institute, De Bilt, Netherlands.



Effects of the 2004 El Niño on tropospheric ozone and water vapor

S. Chandra,^{1,2} J. R. Ziemke,^{1,2} M. R. Schoeberl,³ L. Froidevaux,⁴ W. G. Read,⁴ P. F. Levelt,⁵ and P. K. Bhartia³

Received 14 November 2006; revised 13 December 2006; accepted 3 January 2007; published 21 March 2007.

[1] The global effects of the 2004 El Niño on tropospheric ozone and H₂O based on Aura OMI and MLS measurements are analyzed. Although it was a weak El Niño from a historical perspective, it produced significant changes in these parameters in tropical latitudes. Tropospheric ozone increased by 10–20% over most of the western Pacific region and decreased by about the same amount over the eastern Pacific region. H₂O in the upper troposphere showed similar changes but with opposite sign. These zonal changes in tropospheric ozone and H₂O are caused by the eastward shift in the Walker circulation in the tropical Pacific region during El Niño. During the 2004 El Niño, biomass burning did not have a significant effect on the ozone budget in the troposphere, unlike the 1997 El Niño. Zonally averaged tropospheric column ozone did not change significantly either globally or over tropical latitudes. **Citation:** Chandra, S., J. R. Ziemke, M. R. Schoeberl, L. Froidevaux, W. G. Read, P. F. Levelt, and P. K. Bhartia (2007), Effects of the 2004 El Niño on tropospheric ozone and water vapor, *Geophys. Res. Lett.*, *34*, L06802, doi:10.1029/2006GL028779.

1. Introduction

[2] Ziemke and Chandra [2003] have shown that El Niño and La Niña events are major sources of decadal variability in tropospheric O₃ in the tropical atmosphere. These events produce changes in the convection pattern and large-scale circulation in the tropical Pacific region causing tropospheric column ozone (TCO) to vary from the western to the eastern Pacific with a sign change near the dateline. During El Niño, TCO is enhanced over the Indonesian region and reduced over the eastern Pacific. La Niña generally produces the opposite effect. One of the most intense El Niño events on record occurred during 1997 which caused a major perturbation in the ocean-atmosphere system including a drought and large-scale forest fires in the Indonesian region. The effects of the 1997 El Niño on tropospheric O₃ in the tropics have been extensively studied from both satellite and ground based measurements [e.g., Chandra *et al.*, 1998, 2002; Fujiwara *et al.*, 1999; Thompson *et al.*, 2001] and are, generally, well simulated by global models of

atmospheric chemistry and transport [e.g., Sudo and Takahashi, 2001; Chandra *et al.*, 2002; Peters *et al.*, 2001, Zeng and Pyle, 2005, Doherty *et al.*, 2006]. The study of El Niño and La Niña related changes in tropospheric O₃ has been generally limited to the tropical region because global measurements of tropospheric O₃ outside the tropics were not available. A number of studies have suggested that El Niño has significant influence on the inter-annual variation of stratosphere-troposphere exchange (STE) which affects tropospheric O₃ outside the tropics [Langford *et al.*, 1998; James *et al.*, 2003; Zeng and Pyle, 2005].

[3] Recently, Ziemke *et al.* [2006] produced global maps of TCO from the Aura Ozone Monitoring Instrument (OMI) and Microwave Limb Sounder (MLS) measurements beginning August 2004. TCO is determined using the tropospheric O₃ residual method which involves subtracting stratospheric column ozone (SCO) from total column ozone measured from MLS and OMI instruments. There was an El Niño event during the latter part of 2004. Even though this event was weak by historical standards, it provides an opportunity to study the possible effects of El Niño on tropospheric O₃ outside the tropical region. The purpose of this paper is to study global effects of the 2004 El Niño on tropospheric O₃ derived from the OMI/MLS instruments on the Aura Satellite. This study combines tropospheric O₃ measurements with H₂O measurements from the MLS instrument on the same satellite. Like O₃, H₂O is affected by deep tropical convection and large-scale transport processes. During 1997, El Niño-related changes in tropospheric O₃ and upper troposphere (UT) H₂O were anti-correlated over most of the tropical region [Chandra *et al.*, 1998].

2. The 2004 El Niño Event

[4] According to the World Meteorological Organization (WMO) criterion (available at <http://www.nws.noaa.gov/ost/climate/STIP/ElNinoDef.htm>), an El Niño event occurs when the sea surface temperature (SST) in the Niño 3.4 region (a rectangular region covering longitudes 120°W–170°W and latitudes 5°S–5°N) is at least 0.5°C above normal when averaged over three consecutive months. Using this criterion, the last six months of 2004 may be categorized as El Niño months. The mean values of SST in these months were 0.7°C to 0.9°C higher with respect to 1971–2000 base periods (available at http://www.cpc.noaa.gov/products/analysis_monitoring/ensostuff/ensoyears.shtml). The SST values are lower compared to the 2002 El Niño and significantly lower compared to the 1997 El Niño. For example, the mean SST anomalies (ΔSST) for November and December 2004 were respectively 0.9°C and 0.8°C. For the same two months, ΔSST were 1.5°C for the 2002 El Niño, and 2.5°C for the 1997 El Niño. In all cases, the mean represents a three-month

¹Goddard Earth Sciences and Technology, University of Maryland Baltimore County, Baltimore, Maryland, USA.

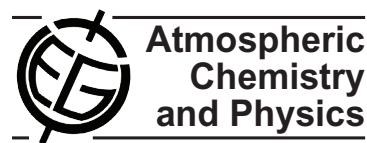
²Also at NASA Goddard Space Flight Center, Greenbelt, Maryland, USA.

³NASA Goddard Space Flight Center, Greenbelt, Maryland, USA.

⁴Jet Propulsion Laboratory, California Institute of Technology, Pasadena, California, USA.

⁵Royal Netherlands Meteorological Institute, De Bilt, Netherlands.

Atmos. Chem. Phys., 7, 5501–5517, 2007
 www.atmos-chem-phys.net/7/5501/2007/
 © Author(s) 2007. This work is licensed
 under a Creative Commons License.



Intercontinental transport of pollution and dust aerosols: implications for regional air quality

Mian Chin¹, T. Diehl², P. Ginoux³, and W. Malm⁴

¹NASA Goddard Space Flight Center, Greenbelt, MD, USA

²University of Maryland Baltimore County, Baltimore, MD, USA

³NOAA Geophysical Fluid Dynamics Laboratory, Princeton, NJ, USA

⁴National Park Service, CIRA, Colorado State University, Fort Collins, CO, USA

Received: 8 June 2007 – Published in Atmos. Chem. Phys. Discuss.: 26 June 2007

Revised: 4 October 2007 – Accepted: 8 October 2007 – Published: 1 November 2007

Abstract. We use the global model GOCART to examine the impact of pollution and dust aerosols emitted from their major sources on surface fine particulate matter concentrations at regional and hemispheric scales. Focusing on the North America region in 2001, we use measurements from the IMPROVE network in the United States to evaluate the model-simulated surface concentrations of the “reconstructed fine mass” (RCFM) and its components of ammonium sulfate, black carbon (BC), organic matter (OM), and fine mode dust. We then quantify the RCFM budget in terms of the RCFM chemical composition, source type, and region of origin to find that in the eastern U.S., ammonium sulfate is the dominant RCFM component (~60%) whereas in the western U.S., dust and OM are just as important as sulfate but have considerable seasonal variations, especially in the NW. On an annual average, pollution aerosol (defined as aerosols from fuel combustion for industrial and transportation uses) from North America accounts for 65–70% of the surface RCFM in the eastern U.S. and for a lower proportion of 30–40% in the western U.S.; by contrast, pollution from outside of North America contributes to just 2–6% ($\sim 0.2 \mu\text{g m}^{-3}$) of the total RCFM over the U.S. In comparison, long-range transport of dust brings 3 to 4 times more fine particles than the transport of pollution to the U.S. ($0.5\text{--}0.8 \mu\text{g m}^{-3}$ on an annual average) with a maximum influence in spring and over the NW. Of the major pollution regions, Europe has the largest potential to affect the surface aerosol concentrations in other continents due to its shorter distance from receptor continents and its larger fraction of sulfate-producing precursor gas in the outflow. With the IPCC emission scenario for the year 2000, we find that European emissions increase levels of ammonium sulfate by $1\text{--}5 \mu\text{g m}^{-3}$ over the surface of northern Africa and western Asia, and its contribution to eastern Asia

($\geq 0.2 \mu\text{g m}^{-3}$) is twice as much as the Asian contribution to North America. Asia and North America pollution emissions exert strong impacts on their neighboring oceans, but their influences over other continents are relatively small ($\leq 10\%$) due to long traveling distances across the oceans and efficient removal during transport. Among the major dust source regions, Asia displays a significant influence over large areas in the northern hemisphere except over the North Atlantic and the tropics, where African dust dominates. We also notice that the African dust and European pollution can travel eastward through a pathway spanning across Asia and North Pacific to western North America; such a pathway is difficult to detect because these aerosols usually merge and travel together with Asian dust and pollution labeled as “Asian outflow”.

1 Introduction

Aerosol, also known as particulate matter (PM), is one of the major air pollutants determining ambient air quality. Airborne particle sizes vary widely from a few nm (10^{-9} m) to a few hundred μm in diameter; those with diameters smaller than $10 \mu\text{m}$ (PM_{10}) are of health concern because they can penetrate into the lungs, and those smaller than $2.5 \mu\text{m}$ ($\text{PM}_{2.5}$) pose the most serious risks to human health, being linked to respiratory or cardiovascular diseases and even deaths (Ostro et al., 1999, 2000; World Health Organization, 2002; Pope, 2002). Aerosol is also known to cause regional haze, which leads to discoloration, loss of texture, and deterioration of visual range in national parks and wilderness areas (Malm et al., 2000). Sources of PM include both direct emissions and chemical transformations of precursor gases emitted from power plants, automobiles, wood

Correspondence to: Mian Chin
 (mian.chin@nasa.gov)

Published by Copernicus Publications on behalf of the European Geosciences Union.



Global budget of CO, 1988–1997: Source estimates and validation with a global model

B. N. Duncan,^{1,2,3} J. A. Logan,¹ I. Bey,^{1,4} I. A. Megretskaya,¹ R. M. Yantosca,¹
P. C. Novelli,⁵ N. B. Jones,^{6,7} and C. P. Rinsland⁸

Received 25 January 2007; revised 25 May 2007; accepted 7 August 2007; published 17 November 2007.

[1] We present a model study of carbon monoxide for 1988–1997 using the GEOS-Chem 3-D model driven by assimilated meteorological data, with time-varying emissions from biomass burning and from fossil fuel and industry, overhead ozone columns, and methane. The hydroxyl radical is calculated interactively using a chemical parameterization to capture chemical feedbacks. We document the inventory for fossil fuels/industry and discuss major uncertainties and the causes of differences with other inventories that give significantly lower emissions. We find that emissions hardly change from 1988 to 1997, as increases in Asia are offset by decreases elsewhere. The model reproduces the 20% decrease in CO at high northern latitudes and the 10% decrease in the North Pacific, caused primarily by the decrease in European emissions. The model compares well with observations at sites impacted by fossil fuel emissions from North America, Europe, and east Asia suggesting that the emissions from this source are reliable to 25%, and we argue that bottom-up emission estimates are likely to be too low rather than too high. The model is too low at the seasonal maximum in spring in the southern tropics, except for locations in the Atlantic Ocean. This problem may be caused by an overestimate of the frequency of tropical deep convection, a common problem in models that use assimilated meteorological data. We argue that the yield of CO from methane oxidation is near unity, contrary to some other studies, based on removal rates of intermediate species.

Citation: Duncan, B. N., J. A. Logan, I. Bey, I. A. Megretskaya, R. M. Yantosca, P. C. Novelli, N. B. Jones, and C. P. Rinsland (2007), Global budget of CO, 1988–1997: Source estimates and validation with a global model, *J. Geophys. Res.*, 112, D22301, doi:10.1029/2007JD008459.

1. Introduction

[2] Carbon monoxide plays important roles in atmospheric chemistry. Reaction with carbon monoxide (CO) provides the dominant sink for the hydroxyl radical (OH), the main tropospheric oxidant, and oxidation of CO provides a source or a sink for ozone, depending on levels of nitrogen oxides (NO_x) [e.g., Levy, 1971; Crutzen, 1973; Logan et al., 1981]. Changes in emissions of CO have the potential to influence climate by affecting methane and other radiatively important gases that are removed by OH, and by affecting tropospheric ozone itself [e.g., Daniel and Solomon, 1988; Mickley et al., 1999].

[3] Carbon monoxide increased in the Northern Hemisphere (NH) from the 1950s until the 1980s and decreased from the late 1980s until mid-1997 [Zander et al., 1989;

Khalil and Rasmussen, 1994; Novelli et al., 1994, 1998, 2003]. There were large increases in CO in the NH associated with anomalously large forest fires in 1998, 2002, and 2003; however, levels in 2000 and 2001 were similar to those in 1997 [Novelli et al., 2003; Yurganov et al., 2004, 2005]. Part of the downward trend in CO in the early 1990s has been attributed to the effects of the Mount Pinatubo eruption in June 1991, when ozone levels in the lower stratosphere were reduced and tropospheric OH was enhanced [Bekki et al., 1994; Novelli et al., 1994; Dlugokencky et al., 1996].

[4] The temporal behavior of CO is best documented by surface measurements from the NOAA Earth System Research Laboratory, Global Monitoring Division (GMD) that started in 1988 [Novelli et al., 1994, 1998, 2003], and by column measurements at a few locations [e.g., Mahieu et

¹School of Engineering and Applied Sciences, Harvard University, Cambridge, Massachusetts, USA.

²Now at Goddard Earth Sciences and Technology Center, University of Maryland, Baltimore County, Baltimore, Maryland, USA.

³Also at NASA Goddard Space Flight Center, Greenbelt, Maryland, USA.

Copyright 2007 by the American Geophysical Union.
0148-0227/07/2007JD008459\$09.00

⁴Now at Laboratoire de Modélisation de Chimie Atmosphérique, École Polytechnique Fédérale de Lausanne, Lausanne, Switzerland.

⁵Global Monitoring Division, Earth System Research Laboratory, NOAA, Boulder, Colorado, USA.

⁶National Institute of Water and Atmospheric Research, Lauder, New Zealand.

⁷Now at Department of Chemistry, University of Wollongong, Wollongong, New South Wales, Australia.

⁸NASA Langley Research Center, Hampton, Virginia, USA.



Mesospheric dynamical changes induced by the solar proton events in October–November 2003

Charles H. Jackman,¹ Raymond G. Roble,² and Eric L. Fleming^{1,3}

Received 29 September 2006; revised 2 January 2007; accepted 17 January 2007; published 27 February 2007.

[1] The Thermosphere Ionosphere Mesosphere Electrodynamic General Circulation Model (TIME-GCM) was used to study the atmospheric dynamical influence of the solar protons that occurred in Oct–Nov 2003, the fourth largest period of solar proton events (SPEs) measured in the past 40 years. The highly energetic solar protons produced odd hydrogen (HO_x) and odd nitrogen (NO_y). Significant short-lived ozone decreases (10–70%) followed these enhancements of HO_x and NO_y and led to a cooling of most of the lower mesosphere. Temperature changes up to ±2.6 K were computed as well as wind (zonal, meridional, vertical) perturbations up to 20–25% of the background winds as a result of the solar protons. The solar proton-induced mesospheric temperature and wind perturbations diminished over a period of 4–6 weeks after the SPEs. The Joule heating in the mesosphere, induced by the solar protons, was computed to be relatively insignificant for these solar storms. **Citation:** Jackman, C. H., R. G. Roble, and E. L. Fleming (2007), Mesospheric dynamical changes induced by the solar proton events in October–November 2003, *Geophys. Res. Lett.*, 34, L04812, doi:10.1029/2006GL028328.

1. Introduction

[2] Several very large solar eruptive events in late October and early November 2003 resulted in huge fluxes of charged particles at the Earth [Mewaldt *et al.*, 2005]. Much of the energy was carried by solar protons, which impacted the middle atmosphere (stratosphere and mesosphere) leading to ionizations, dissociations, dissociative ionizations, and excitations. The proton-induced atmospheric interactions resulted in the production of odd hydrogen, HO_x (H, OH, HO₂), and odd nitrogen, NO_y (N, NO, NO₂, NO₃, N₂O₅, HNO₃, HO₂NO₂, HONO, ClONO₂, ClNO₂, BrONO₂) constituents either directly or through a photochemical sequence [e.g., Swider and Keneshea, 1973; Crutzen *et al.*, 1975]. There were a few periods from 26 Oct.–7 Nov., 2003, when the proton fluxes increased dramatically beyond background levels for 1–3 days. These periods are known as solar proton events (SPEs) and some of the middle atmospheric constituent influences during these SPEs have been discussed before [e.g., Jackman *et al.*, 2005a; Verronen *et al.*, 2005]. These Oct./Nov. 2003 SPEs were very intense

and were computed to be the fourth largest SPE period in the past 40 years [Jackman *et al.*, 2005b].

[3] We are not aware of any measured atmospheric dynamical changes during these very significant atmospheric perturbations, however, past studies [Banks, 1979; Reagan *et al.*, 1981; Jackman and McPeters, 1985; Roble *et al.*, 1987; Reid *et al.*, 1991; Zadorozhny *et al.*, 1994; Jackman *et al.*, 1995; Krivolutsky *et al.*, 2006] have suggested that very large SPEs can lead to temperature changes through ozone depletion and/or Joule heating.

[4] In this paper, we used the latest version of the TIME-GCM (Thermosphere Ionosphere Mesosphere Electrodynamic – General Circulation Model) [Roble, 2000], which contains both ozone photochemistry and auroral particle and Joule heating, to study the influence of the very large proton fluxes during Oct./Nov. 2003 on the temperature and winds of the middle atmosphere. The TIME-GCM allowed us the opportunity to compare and contrast the different atmospheric perturbations during SPEs that lead to temperature and wind changes. We will focus on a snap-shot output from the model for one day, 30 October 2003, at 0:00 UT near a period of maximum solar proton flux to investigate these effects.

2. Model Description and Solar Proton Caused Constituent Change

[5] The TIME-GCM was first described by Roble and Ridley [1994]. This model has an effective 5° latitude × 5° longitude grid with 45 constant pressure surfaces in the vertical between approximately 30 and 500 km altitude with a vertical resolution of 2 grid points per scale height and a model time step of 5 minutes. The TIME-GCM has a comprehensive set of physical, chemical, and dynamical processes included to simulate the upper atmosphere and ionosphere. A detailed description of the model and its components is given by Roble [2000].

[6] The model is forced at its lower boundary of 10 hPa by global geopotential height and temperature distributions from NCEP (National Centers of Environmental Prediction) analysis. This feature provides the ability to simulate particular periods of interest, such as 27 October through 11 December 2003 for this specific study [e.g., Liu and Roble, 2005].

[7] We use the proton flux data provided by the National Oceanic and Atmospheric Administration (NOAA) Space Environment Center (SEC) for the NOAA Geostationary Operational Environmental Satellites (GOES) (see <http://sec.noaa.gov/Data/goes.html>). The GOES 11 data are considered to be the most reliable of the current GOES datasets for the proton fluxes depositing energy into polar latitudes and were used as the source of protons in several

¹NASA Goddard Space Flight Center, Greenbelt, Maryland, USA.

²High Altitude Observatory, National Center for Atmospheric Research, Boulder, Colorado, USA.

³Also at Science Systems and Applications, Inc., Lanham, Maryland, USA.



Effects of data selection and error specification on the assimilation of AIRS data[†]

J. Joiner,^{1*} E. Brin,² R. Treadon,³ J. Derber,³ P. Van Delst,³ A. Da Silva,⁴ J. Le Marshall,³ P. Poli,⁵ R. Atlas,⁶ D. Bungato² and C. Cruz⁷

¹ NASA Goddard Space Flight Center Laboratory for Atmospheres, USA

² Science Applications International Corporation, USA

³ Joint Center for Satellite Data Assimilation, USA

⁴ NASA Goddard Space Flight Center Global Modeling and Assimilation Office, USA

⁵ Centre National de Recherches Météorologiques, Météo France, Toulouse, France

⁶ NOAA Atlantic Oceanographic and Meteorological Laboratory, USA

⁷ NGITI, USA

ABSTRACT: The Atmospheric InfraRed Sounder (AIRS), flying aboard NASA's Aqua satellite with the Advanced Microwave Sounding Unit-A (AMSU-A) and four other instruments, has been providing data for use in numerical weather prediction and data assimilation systems for over three years. The full AIRS data set is currently not transmitted in near-real-time to the prediction/assimilation centres. Instead, data sets with reduced spatial and spectral information are produced and made available within three hours of the observation time. In this paper, we evaluate the use of different channel selections and error specifications. We achieve significant positive impact from the Aqua AIRS/AMSU-A combination during our experimental time period of January 2003. The best results are obtained using a set of 156 channels that do not include any in the H₂O band between 1080 and 2100 cm⁻¹. The H₂O band channels have a large influence on both temperature and humidity analyses. If observation and background errors are not properly specified, the partitioning of temperature and humidity information from these channels will not be correct, and this can lead to a degradation in forecast skill. Therefore, we suggest that it is important to focus on background error specification in order to maximize the impact from AIRS and similar instruments. In addition, we find that changing the specified channel errors has a significant effect on the amount of data that enters the analysis as a result of quality control thresholds that are related to the errors. However, moderate changes to the channel errors do not significantly impact forecast skill with the 156 channel set. We also examine the effects of different types of spatial data reduction on assimilated data sets and NWP forecast skill. Whether we pick the centre or the warmest AIRS pixel in a 3×3 array affects the amount of data ingested by the analysis but does not have a statistically significant impact on the forecast skill. Published in 2007 by John Wiley & Sons, Ltd.

KEY WORDS forecast; numerical; weather; climate; radiances; satellite

Received 5 May 2006; Revised 20 September 2006; Accepted 18 October 2006

1. Introduction

The Atmospheric Infra-Red Sounder (AIRS) (Aumann *et al.*, 2003) is the first of several advanced high-spectral-resolution nadir-viewing passive infrared sounders to be used for climate applications and operational numerical weather prediction (NWP). AIRS is a grating spectrometer that has been flying on the National Aeronautics and Space Administration's (NASA) Earth Observing System (EOS) polar-orbiting Aqua platform since May 2002 along with the Advanced Microwave Sounding Unit - A (AMSU-A) and four other instruments. Over the next few years, additional kilochannel interferometers will fly in Low Earth Orbit. These include the Infrared Atmospheric

Sounding Interferometer (IASI) on the EUMETSAT MetOp platform and the Cross-Track Infrared Sounder (CrIS) on the National Polar-orbiting Operational Environmental Satellite System (NPOESS) series of satellites as well as the NASA/National Oceanic and Atmospheric Administration (NOAA)/(US) Department of Defense (DoD) NPOESS Preparatory Project (NPP).

In order to facilitate near-real-time (NRT) transmission of the voluminous AIRS data, the complete AIRS data set must be reduced. There are several possible methods of data reduction. These include channel and/or pixel subsetting and methods such as principle component analysis that represent only the most important modes of the spectral information content. Before launch, the NOAA National Environmental Satellite Data and Information Service (NESDIS) set up a special processing system to provide several different data sets to the NWP and data assimilation community (Goldberg *et al.*, 2003).

* Correspondence to: J. Joiner, NASA Goddard Space Flight Center, Code 613.3, Greenbelt, MD, 20771, USA.
 E-mail: Joanna.Joiner@nasa.gov

[†] This article is a US Government work and is in the public domain in the USA.



Variations in stratospheric inorganic chlorine between 1991 and 2006

D. J. Lary,^{1,2} D. W. Waugh,³ A. R. Douglass,² R. S. Stolarski,² P. A. Newman,² and H. Mussa⁴

Received 16 March 2007; revised 28 August 2007; accepted 21 September 2007; published 13 November 2007.

[1] A consistent time series of stratospheric inorganic chlorine Cl_y from 1991 to present is formed using spaceborne observations together with neural networks. A neural network is first used to account for inter-instrument biases in HCl observations. A second neural network is used to learn the abundance of Cl_y as a function of HCl and CH_4 , and to form a time series using available HCl and CH_4 measurements. The estimates of Cl_y are broadly consistent with calculations based on tracer fractional releases and previous estimates of stratospheric age of air. These new estimates of Cl_y provide a critical test for global models, which exhibit significant differences in predicted Cl_y and ozone recovery. **Citation:** Lary, D. J., D. W. Waugh, A. R. Douglass, R. S. Stolarski, P. A. Newman, and H. Mussa (2007), Variations in stratospheric inorganic chlorine between 1991 and 2006, *Geophys. Res. Lett.*, *34*, L21811, doi:10.1029/2007GL030053.

1. Introduction

[2] Knowledge of the distribution of inorganic chlorine Cl_y in the stratosphere is needed to attribute changes in stratospheric ozone to changes in halogens, and to assess the realism of chemistry-climate models [Eyring *et al.*, 2006; Eyring *et al.*, 2007]. However, there are limited direct observations of Cl_y . Simultaneous measurements of the major inorganic chlorine species are rare [Zander *et al.*, 1992; Gunson *et al.*, 1994; Bonne *et al.*, 2000; Nassar *et al.*, 2006]. In the upper stratosphere, Cl_y can be inferred from HCl alone [e.g., Anderson *et al.*, 2000; Froidevaux *et al.*, 2006b].

[3] Here we combine observations from several spaceborne instruments using neural networks [Lary and Mussa, 2004] to produce a time series for Cl_y . A neural network is used to characterize differences among various HCl measurements, and to perform an inter-instrument bias correction. Measurements from several different instruments are used in this analysis. These instruments, together with temporal coverage and measurement uncertainties, are listed in Table 1. The HALOE uncertainties are only estimates of random error and do not include any indications of overall accuracy. All instruments provide measurements through the depth of the stratosphere. A second neural network is

used to infer Cl_y from these corrected HCl measurements and measurements of CH_4 .

[4] Sections 2 and 3 describe the HCl and Cl_y intercomparisons. Section 4 presents a summary.

2. HCl Intercomparison

[5] We first compare measurements of HCl from the different instruments listed in Table 1. Comparisons are made in equivalent PV latitude - potential temperature coordinates [Schoeberl *et al.*, 1989; Proffitt *et al.*, 1989; Lait *et al.*, 1990; Douglass *et al.*, 1990; Lary *et al.*, 1995; Schoeberl *et al.*, 2000] to extend the effective latitudinal coverage of the measurements and identify contemporaneous measurements in similar air masses.

[6] The Halogen Occultation Experiment (HALOE) provides the longest record of space based HCl observations. Figure 1 compares HALOE HCl with HCl observations from (1) the Atmospheric Trace Molecule Spectroscopy Experiment (ATMOS), (2) the Atmospheric Chemistry Experiment (ACE), and (3) the Microwave Limb Sounder (MLS). In these plots each point is the median HCl observation made by the instrument during each month for 30 equivalent latitude bins from pole to pole and 25 potential temperature bins from the 300–2500 K potential temperature surfaces.

[7] For each of these bins we only use data in the range where the supplied quality flags show it suitable for scientific use. For each bin, we characterize the median observation uncertainty and the representativeness uncertainty. The representativeness is a measure of the spatial variability over the bin, in our case characterized by the average deviation of the observations in the bin. The average deviation is a measure of the width of the probability distribution of observations. Unlike the standard deviation, the average deviation is not strongly influenced by a few outliers. Each of these uncertainties are used later in Figures 2 and 3.

[8] A consistent picture is seen in these plots: HALOE HCl measurements are lower than those from the other instruments. The slopes of the linear fits (relative scaling) are 1.05 for the HALOE-ATMOS comparison, 1.09 for the HALOE-MLS, and 1.18 for the HALOE-ACE. The offsets are apparent at the 525 K isentropic surface and above. Previous comparisons among HCl datasets reveal a similar bias for HALOE [Russell *et al.*, 1996; McHugh *et al.*, 2005; Froidevaux *et al.*, 2006a]. ACE and MLS HCl measurements are in much better agreement (Figure 1d). Note, all measurements agree within the stated observational uncertainties summarized in Table 1.

[9] To combine the above HCl measurements to form a continuous time series of HCl (and then Cl_y) from 1991 to 2006 it is necessary to account for the biases between data

¹Goddard Earth Sciences and Technology Center, University of Maryland Baltimore County, Baltimore, Maryland, USA.

²Atmospheric Chemistry and Dynamics Branch, NASA Goddard Space Flight Center, Greenbelt, Maryland, USA.

³Department of Earth and Planetary Sciences, Johns Hopkins University, Baltimore, Maryland, USA.

⁴Department of Chemistry, University of Cambridge, Cambridge, UK.

The QBO as potential amplifier and conduit to lower altitudes of solar cycle influence

H. G. Mayr¹, J. G. Mengel², C. L. Wolff¹, F. T. Huang³, and H. S. Porter⁴

¹Goddard Space Flight Center, Greenbelt, MD, USA

²Science Systems & Applications, Lanham, MD, USA

³Creative Computing Solutions Inc. Rockville, MD, USA

⁴Furman University, Greenville, SC, USA

Received: 6 April 2006 – Revised: 2 March 2007 – Accepted: 13 April 2007 – Published: 4 June 2007

Abstract. In several papers, the solar cycle (SC) effect in the lower atmosphere has been linked observationally to the Quasi-biennial Oscillation (QBO) of the zonal circulation. Salby and Callaghan (2000) in particular analyzed the QBO wind measurements, covering more than 40 years, and discovered that they contain a large SC signature at 20 km. We present here the results from a study with our 3-D Numerical Spectral Model (NSM), which relies primarily on parameterized gravity waves (GW) to describe the QBO. In our model, the period of the SC is taken to be 10 years, and the relative amplitude of radiative forcing varies exponentially with height, i.e., 0.2% at the surface, 2% at 50 km, and 20% at 100 km and above. Applying spectral analysis to identify the SC signature, the model generates a relatively large modulation of the QBO, which reproduces the observations qualitatively. The numerical results demonstrate that the QBO modulation, closely tracking the phase of the SC, is robust and persists at least for 70 years. The question is what causes the SC effect, and our analysis shows that four interlocking processes are involved: (1) In the mesosphere at around 60 km, the solar UV variations generate in the zonal winds a SC modulation of the 12-month annual oscillation, which is hemispherically symmetric and confined to equatorial latitudes like the QBO. (2) Although the amplitude of this equatorial annual oscillation (EAO) is relatively small, its SC modulation is large and extends into the lower stratosphere under the influence of, and amplified by, wave forcing. (3) The amplitude modulations of both EAO and QBO are essentially in phase with the imposed SC heating for the entire time span of the model simulation. This indicates that, due to positive feedback in the wave mechanism, the EAO apparently provides the pathway and pacemaker for the SC modulation of the QBO. (4) Our analysis demonstrates that the SC modulations of the QBO and EAO are ampli-

fied by tapping the momentum from the upward propagating gravity waves. Influenced and amplified by wave processes, the QBO thus acts as conduit to transfer to lower altitudes the larger SC variations in the UV absorbed in the mesosphere. Our model produces in the temperature variations of the QBO and EAO measurable SC modulations at polar latitudes near the tropopause. The effects are apparently generated by the meridional circulation, and planetary waves presumably, which redistribute the energy from the equatorial region where the waves are very effective in amplifying the SC influence.

Keywords. Meteorology and atmospheric dynamics (General circulation; Middle atmosphere dynamics; Waves and tides)

1 Introduction

The Quasi-biennial Oscillation (QBO) of the zonal circulation at equatorial latitudes has been linked observationally to solar cycle (SC) effects in the stratosphere at northern polar latitudes. Following a study by Holton and Tan (1980), Labitzke (1982, 1987) and Labitzke and van Loon (1988, 1992) discovered that the temperatures at northern polar latitudes in winter are positively and negatively correlated with the SC when the QBO is respectively in its negative and positive phase. And at mid-latitudes they observed opposite correlations. In the northern stratosphere, Dunkerton and Baldwin (1992) and Baldwin and Dunkerton (1998) also found evidence of a correlation between the SC and the phase of the QBO.

The SC influence on the QBO connection with the polar region has been simulated successfully in recent modeling studies. Matthes et al. (2004) inserted rocketsonde data into their GCM to produce realistic QBO wind fields around the equator. Carrying out model runs with fixed eastward and

Correspondence to: H. G. Mayr
(hmayr2@verizon.net)



Ozone climatological profiles for satellite retrieval algorithms

Richard D. McPeters,¹ Gordon J. Labow,² and Jennifer A. Logan³

Received 24 January 2005; revised 10 October 2006; accepted 8 December 2006; published 14 March 2007.

[1] A new altitude-dependent ozone climatology has been produced for use with the version 8 Total Ozone Mapping Spectrometer (TOMS) and Solar Backscatter Ultraviolet retrieval algorithms. The climatology consists of monthly average ozone profiles for 10° latitude zones covering altitudes from 0 to 60 km (in Z^* pressure altitude coordinates). The climatology was formed by combining data from Stratospheric Aerosol and Gas Experiment II (SAGE II; 1988–2001) or Microwave Limb Sounder (MLS; 1991–1999) with data from balloon sondes (1988–2002). Ozone below 10 km is based on balloon sondes, whereas ozone at 19 km and above is based on SAGE II measurements. When SAGE data are not available (at high latitudes), MLS data are used. The ozone climatology in the southern hemisphere and tropics has been greatly improved in recent years by the addition of a large number of balloon sonde measurements made under the Southern Hemisphere Additional Ozonesondes program. The new climatology better represents the seasonal behavior of ozone in the troposphere, including the known hemispheric asymmetry, and in the upper stratosphere. A modification of this climatology was used for the TOMS version 8 retrieval that includes total ozone dependence, which is important in the lower stratosphere. Comparisons of TOMS ozone with ground stations show improved accuracy over previous TOMS retrievals due in part to the new climatology.

Citation: McPeters, R. D., G. J. Labow, and J. A. Logan (2007), Ozone climatological profiles for satellite retrieval algorithms, *J. Geophys. Res.*, 112, D05308, doi:10.1029/2005JD006823.

1. Introduction

[2] Ozone climatologies are used for many purposes, and no single climatology will be optimum for all uses. A climatology developed by *Fortuin and Kelder* [1998] based on a combination of balloon and Solar Backscatter Ultraviolet (SBUV) data was, they note, intended mainly for climate simulations with general circulation models. *McPeters et al.* [1997] developed a climatology using SBUV data specifically for estimating the amount of ozone above balloon burst altitude so that total column ozone could be calculated from electrochemical concentration cell sonde measurements. Recently, *Lamsal et al.* [2004] developed a climatology to be used as an a priori for the Sciamachy optimal retrieval algorithm that has also been used in differential optical absorption spectroscopy retrievals. This climatology uses total column ozone to parameterize the profile shape.

[3] Satellite retrieval algorithms for backscattered ultraviolet (BUV) measurements have in the past used a relatively simple ozone climatology. The Total Ozone Mapping Spectrometer (TOMS) retrievals in version 7 used a total

ozone-dependent climatology consisting of 26 profiles with ozone in Umkehr layers (~5 km) covering low-latitude, midlatitude, and high-latitude zones. That climatology and results of a study of the errors due to profile shape at high latitudes are discussed by *Wellemeyer et al.* [1997]. While such a climatology is adequate for accounting for stratospheric ozone profile shape changes, it has a relatively fixed tropospheric ozone climatology since tropospheric ozone does not correlate well with total column ozone. This has become a limitation on accuracy since tropospheric ozone variability has proven to be one of the largest sources of error in the current algorithms. These errors are discussed by *Bhartia* [2002] in the OMI Algorithm Theoretical Basis Document (ATBD).

[4] Ozone retrieval algorithms based on the optimal retrieval method [*Rodgers*, 2000] benefit from an accurate climatology in altitude regions where the measurement loses sensitivity, for example, in the lowest 10 km of the atmosphere for a TOMS total column ozone retrieval. The climatology also supplies information to such retrievals in the form of higher vertical resolution information than the retrieval itself can achieve. An SBUV retrieval derives a fairly accurate measure of the total amount of ozone between the ground and about 20 km, but has little information on how it is distributed. The climatology determines the distribution of ozone within this region in an SBUV retrieval.

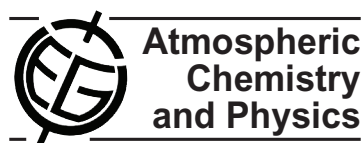
[5] A good climatology can also be used when detailed day-to-day information is not necessary, such as in the

¹Laboratory for Atmospheres, NASA Goddard Space Flight Center, Greenbelt, Maryland, USA.

²Science Systems and Applications Inc., Lanham, Maryland, USA.

³Division of Engineering and Applied Science, Harvard University, Cambridge, Massachusetts, USA.

Atmos. Chem. Phys., 7, 2435–2445, 2007
 www.atmos-chem-phys.net/7/2435/2007/
 © Author(s) 2007. This work is licensed
 under a Creative Commons License.



Observationally derived transport diagnostics for the lowermost stratosphere and their application to the GMI chemistry and transport model

S. E. Strahan¹, B. N. Duncan¹, and P. Hoor²

¹Goddard Earth Science and Technology Center, University of Maryland, Baltimore County, Baltimore, MD 21250, USA

²Max Planck Institute for Chemistry, Air Chemistry, Mainz, Germany

Received: 8 January 2007 – Published in Atmos. Chem. Phys. Discuss.: 29 January 2007

Revised: 24 April 2007 – Accepted: 27 April 2007 – Published: 11 May 2007

Abstract. Transport from the surface to the lowermost stratosphere (LMS) can occur on timescales of a few months or less, making it possible for short-lived tropospheric pollutants to influence stratospheric composition and chemistry. Models used to study this influence must demonstrate the credibility of their chemistry and transport in the upper troposphere and lower stratosphere (UT/LS). Data sets from satellite and aircraft instruments measuring CO, O₃, N₂O, and CO₂ in the UT/LS are used to create a suite of diagnostics for the seasonally-varying transport into and within the lowermost stratosphere, and of the coupling between the troposphere and stratosphere in the extratropics. The diagnostics are used to evaluate a version of the Global Modeling Initiative (GMI) Chemistry and Transport Model (CTM) that uses a combined tropospheric and stratospheric chemical mechanism and meteorological fields from the GEOS-4 general circulation model. The diagnostics derived from N₂O and O₃ show that the model lowermost stratosphere has realistic input from the overlying high latitude stratosphere in all seasons. Diagnostics for the LMS show two distinct layers. The upper layer begins ~30 K potential temperature above the tropopause and has a strong annual cycle in its composition. The lower layer is a mixed region ~30 K thick near the tropopause that shows no clear seasonal variation in the degree of tropospheric coupling. Diagnostics applied to the GMI CTM show credible seasonally-varying transport in the LMS and a tropopause layer that is realistically coupled to the UT in all seasons. The vertical resolution of the GMI CTM in the UT/LS, ~1 km, is sufficient to realistically represent the extratropical tropopause layer. This study demonstrates that the GMI CTM has the transport credibility required to study the impact of tropospheric emissions on the stratosphere.

Correspondence to: S. E. Strahan
 (sstrahan@pop600.gsfc.nasa.gov)

1 Introduction

Evaluation of transport between the upper troposphere (UT) and lower stratosphere (LS) is important because of the potential for tropospheric pollutants to impact stratospheric composition and chemistry. A decade ago, Ko et al. (1997) proposed that Br_y produced from short-lived species in the tropical UT may contribute to stratospheric halogen loading, and a recent study using BrO measurements and photochemical models supports this hypothesis (Salawitch et al., 2005). More recently, a “tape recorder” of CO forced by seasonal variations in biomass burning was identified in the tropical UT/LS using satellite CO measurements (Schoeberl et al., 2006). Tropospheric pollutants with lifetimes of only a few months can affect the composition of the lowest portions of the stratosphere.

There are two major transport pathways to the stratosphere (Holton et al., 1995; Dessler et al., 1995). In the tropics, convection brings boundary layer air up to ~12 km (~345 K), the base of the tropical tropopause layer (TTL) (Folkins, 2002). The TTL begins where convective mass flux falls off rapidly and extends to the cold point tropopause at 17–18 km (370–380 K) (Gettelman and Forster, 2002). Net heating rates become positive at about 16 km (~360 K) in the TTL and ascent by the Brewer-Dobson circulation slowly lifts air up to and across the tropical tropopause and into the stratosphere. A second pathway involves quasi-horizontal transport of air in the TTL to the extratropical lowermost stratosphere (LMS). This pathway is aided by monsoon anticyclones in the summer hemisphere (Chen, 1995), with poleward transport of tropospheric air on the west side and equatorward transport of stratospheric air on the east side of the monsoonal circulation.

The lowermost stratosphere is defined as the region between the extratropical tropopause, where isentropes connect the stratosphere and troposphere, and the stratospheric

REPORT DOCUMENTATION PAGE

*Form Approved
OMB No. 0704-0188*

The public reporting burden for this collection of information is estimated to average 1 hour per response, including the time for reviewing instructions, searching existing data sources, gathering and maintaining the data needed, and completing and reviewing the collection of information. Send comments regarding this burden estimate or any other aspect of this collection of information, including suggestions for reducing this burden, to Department of Defense, Washington Headquarters Services, Directorate for Information Operations and Reports (0704-0188), 1215 Jefferson Davis Highway, Suite 1204, Arlington, VA 22202-4302. Respondents should be aware that notwithstanding any other provision of law, no person shall be subject to any penalty for failing to comply with a collection of information if it does not display a currently valid OMB control number.

PLEASE DO NOT RETURN YOUR FORM TO THE ABOVE ADDRESS.

1. REPORT DATE (DD-MM-YYYY) 30-05-2008		2. REPORT TYPE Technical Memorandum		3. DATES COVERED (From - To)	
4. TITLE AND SUBTITLE Laboratory for Atmospheres 2007 Technical Highlights				5a. CONTRACT NUMBER	
				5b. GRANT NUMBER	
				5c. PROGRAM ELEMENT NUMBER	
6. AUTHOR(S) Laboratory for Atmospheres				5d. PROJECT NUMBER	
				5e. TASK NUMBER	
				5f. WORK UNIT NUMBER	
7. PERFORMING ORGANIZATION NAME(S) AND ADDRESS(ES) Goddard Space Flight Center Greenbelt, MD 20771				8. PERFORMING ORGANIZATION REPORT NUMBER 200801240	
9. SPONSORING/MONITORING AGENCY NAME(S) AND ADDRESS(ES) National Aeronautics and Space Administration Washington, DC 20546-0001				10. SPONSORING/MONITOR'S ACRONYM(S)	
				11. SPONSORING/MONITORING REPORT NUMBER NASA-TM-2008-214160	
12. DISTRIBUTION/AVAILABILITY STATEMENT Unclassified-Unlimited, Subject Category: 42, 47, 48 Report available from the NASA Center for Aerospace Information, 7115 Standard Drive, Hanover, MD 21076. (301)621-0390					
13. SUPPLEMENTARY NOTES					
14. ABSTRACT The 2007 Technical Highlights describes the efforts of all members of the Laboratory for Atmospheres. Their dedication to advancing Earth Science through conducting research, developing and running models, designing instruments, managing projects, running field campaigns, and numerous other activities, is highlighted in this report.					
15. SUBJECT TERMS Technical Highlights, Laboratory for Atmospheres, Atmospheric Research					
16. SECURITY CLASSIFICATION OF:			17. LIMITATION OF ABSTRACT Unclassified	18. NUMBER OF PAGES 160	19a. NAME OF RESPONSIBLE PERSON Richard W. Stewart
a. REPORT U	b. ABSTRACT U	c. THIS PAGE U			19b. TELEPHONE NUMBER (Include area code) (301) 614-6045